

Motion of Particles in the Vicinity of a Slowly Rotating Black Hole in Hořava-Lifshitz Gravity

by
Tanveer Ahmad



Supervised by
Dr. Ibrar Hussain

Submitted in the partial fulfillment of the

Degree of Master of Philosophy

In

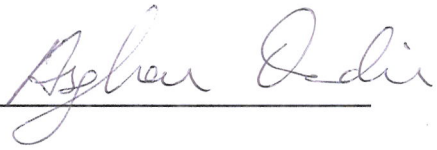
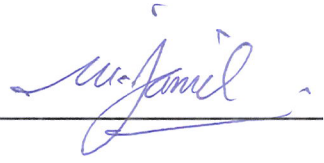
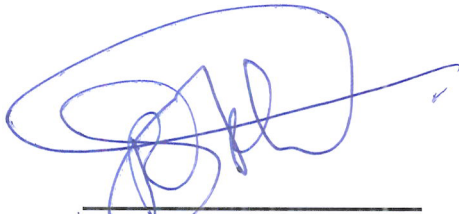
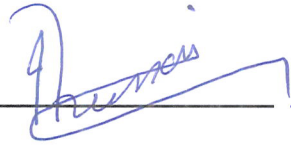
Physics
School of Natural Sciences,

National University of Sciences and Technology,

H-12, Islamabad, Pakistan.

National University of Sciences & Technology**M.Phil THESIS WORK**


We hereby recommend that the dissertation prepared under our supervision by: TANVEER AHMAD, Regn No. NUST201260317MCAMP78112F Titled: Motion of Particles in the Vicinity of a Slowly Rotating Black Hole in the Horava-Lifshitz Gravity be accepted in partial fulfillment of the requirements for the award of **M.Phil** degree.

Examination Committee Members1. Name: Prof. Asghar QadirSignature: 2. Name: Dr. Mubasher JamilSignature: 3. Name: Dr. Sajid AliSignature: 4. Name: Dr. Zahid AhmedSignature: 5. Supervisor: Dr. Ibrar HussainSignature: 

Head of Department

31-08-16

Date

COUNTERSIGNEDDate: 31/8/16

Dean/Principal

*This dissertation is dedicated to my
parents*

for their endless love, support and encouragement.

Contents

1	Introduction	1
1.1	The Metric and Curvature Tensor	4
1.2	The Einstein Field Equations	8
1.3	Notation and Terminology	11
1.4	Black Holes	15
1.4.1	History of Black Holes	16
1.5	Hořava-Lifshitz Gravity	18
1.6	Black Holes in Hořava-Lifshitz Gravity	19
1.7	Particle Dynamics in Black Hole Space-times	20
1.8	Geodesic Equations	22
2	Motion of a Particle in the Vicinity of Static Hořava-Lifshitz Black Holes	24
2.1	Geodesic Motion in Spherically Symmetric Static Spacetime	24
2.2	Timelike Geodesic Motion in Static Hořava-Lifshitz Black Holes	26
2.3	Timelike Geodesics for Static Black Hole in Hořava-Lifshitz Gravity	29

2.3.1	Timelike Geodesic for Radial Motion of Particles in Static Black Hole	30
2.3.2	Timelike Geodesic for Non-radial Motion of Particles in Static Black Hole	32
3	Motion of a Particle in the Vicinity of Slowly Rotating Hořava-Lifshitz Black Hole	35
3.1	Geodesic Motion in Slowly Rotating Spacetime	35
3.2	Timelike Geodesics for Slowly Rotating Black Hole in Hořava-Lifshitz Gravity	38
3.2.1	Timelike Geodesic for Radial Motion of the Particle in Slowly rotating Black Hole	39
3.2.2	Timelike Geodesic for Non-radial Motion of Particles in Slowly Rotating Black Hole	40
3.3	Null Geodesics for Slowly Rotating Black Hole in Hořava-Lifshitz Gravity	46
3.3.1	Null Geodesic for Radial Motion of Particles in Slowly Rotating Black Hole	46
3.3.2	Null Geodesic for Non-radial Motion of Particles in Slowly Rotating Black Hole	48
3.4	Velocity of the Particle	53
3.5	Timelike Geodesics	54
3.5.1	Timelike Geodesic for Radial Motion of the Particle	55
3.5.2	Timelike Geodesic for Non-radial Motion of the Particle	57
3.6	Null Geodesics	58
3.6.1	Null Geodesic for Radial Motion of the Particle	59
3.6.2	Null Geodesic for Non-radial Motion of the Particle	60

4 Conclusion

List of Figures

1.1	Flat Space-time, Courtesy: Google	12
1.2	Curved Space-time, Courtesy: Google	13
1.3	Stable and Unstable Orbits Graph [7]	15
2.1	Plot for the equation (2.3.8) between V_{eff}^2 and r , with parameters $\ell = 0, \omega = 1$ and $M = 1$	31
2.2	Plot of velocity v and distance r for equation (2.3.9) represents the radial motion of the particle with parameters $E = 0.5, \omega = 1$ and $M = 1$	31
2.3	Plot for V_{eff}^2 vs r for equation (2.3.10) for non radial motion of the particle with various values of $\ell^2 = 80M^2, \ell^2 = 40M^2$ and $\ell^2 = 10M^2$ and with parameters $M = 1, \omega = 1$ and $h = 1$	32
2.4	Plot between V_{eff}^2 and r for non radial motion of particles, for various values of $\ell^2 = 80M^2$ and with parameters $M = 1, \omega = 1$ and $h = 1$	33
3.1	Graph for equation (3.2.8) of V_{eff}^2 vs r with parameters $\omega = 1$ and $M = 1$	39
3.2	Graph for equation (3.2.8) of V_{eff}^2 vs r with parameters $\omega = 10$ and $M = 1$	40
3.3	Graph of v vs r for equation (3.2.9) with $\omega = 1, M = 1$ and $E = 0.5$	41
3.4	Graph of v vs r for equation (3.2.9) with $\omega = 10, M = 1$ and $E = 0.5$	41

3.5	Graph for equation (3.2.10) of V_{eff}^2 vs r with parameters $\omega = 1, M = 1, E = 1$ and $\ell^2 = 80M^2$	42
3.6	Graph for equation (3.2.10) of V_{eff}^2 vs r with parameters $\omega = 10, M = 1, E = 1$ and $\ell^2 = 80M^2$	42
3.7	Graph for equation (3.2.10) of V_{eff}^2 vs r with parameters $\omega = 1, M = 1, E = 1$ and $\ell^2 = 40M^2$	43
3.8	Graph for equation (3.2.10) of V_{eff}^2 vs r with parameters $\omega = 10, M = 1, E = 1$ and $\ell^2 = 40M^2$	44
3.9	Graph for equation (3.2.10) of V_{eff}^2 vs r with parameters $\omega = 1, M = 1, E = 1$ and $\ell^2 = 10M^2$	44
3.10	Graph for equation (3.2.10) of V_{eff}^2 vs r with parameters $\omega = 10, M = 1, E = 1$ and $\ell^2 = 10M^2$	45
3.11	Graph of V_{eff}^2 vs r for equation (3.3.1) with parameters $\omega = 1, M = 1, E = 1$ and $\ell^2 = 80M^2$	47
3.12	Graph of V_{eff}^2 vs r for equation (3.3.1) with parameters $\omega = 10, M = 1, E = 1$ and $\ell^2 = 80M^2$	47
3.13	Graph for equation (3.3.4) of V_{eff}^2 vs r with parameters $\omega = 1, M = 1, E = 1$ and $\ell^2 = 80M^2$	48
3.14	Graph for equation (3.3.4) of V_{eff}^2 vs r with parameters $\omega = 10, M = 1, E = 1$ and $\ell^2 = 80M^2$	49
3.15	Graph for equation (3.3.4) of V_{eff}^2 vs r with parameters $\omega = 1, M = 1, E = 1$ and $\ell^2 = 40M^2$	49
3.16	Graph for equation (3.3.4) of V_{eff}^2 vs r with parameters $\omega = 10, M = 1, E = 1$ and $\ell^2 = 40M^2$	50
3.17	Graph for equation (3.3.4) of V_{eff}^2 vs r with parameters $\omega = 1, M = 1, E = 1$ and $\ell^2 = 10M^2$	51
3.18	Graph for equation (3.3.4) of V_{eff}^2 vs r with parameters $\omega = 10, M = 1, E = 1$ and $\ell^2 = 10M^2$	51

3.19	Graph of V_{eff}^2 vs r with parameters $\omega = 1, M = 1, E = 1$ and $\ell^2 = 80M^2$. . .	52
3.20	Graph of V_{eff}^2 vs r with parameters $\omega = 10, M = 1, E = 1$ and $\ell^2 = 80M^2$. . .	53
3.21	Graph of v vs r with parameters $\omega = 1$ and $M = 1$ for equation (3.5.4)	56
3.22	Graph of v vs r with parameters $\omega = 10$ and $M = 1$ for equation (3.5.4)	56
3.23	Graph of v vs r with parameters $\ell = 0.5, \omega = 1, M = 1$ and $E = 1$ and $a = 0.5$ for equation (3.5.5)	57
3.24	Graph of v vs r with parameters $\ell = 0.5, M = 1$ and $E = 1, \omega = 10$ and $a = 0.5$ for equation (3.5.5)	58
3.25	Graph of v vs r with parameters $\omega = 1, M = 1$ for equation (3.6.2)	59
3.26	Graph of v vs r with parameters $\omega = 10, M = 1$ for equation (3.6.2)	60
3.27	Graph of v vs r with parameters $\omega = 1, M = 1, \ell = 0.5$ and $a = 0.5$ for equation (3.6.3)	61
3.28	Graph of v vs r with parameters $\omega = 10, M = 1, \ell = 0.5, \ell = 0.5$ and $a = 0.5$ for equation (3.6.3)	61

Acknowledgements

First of all, I am thankful to Almighty Allah who enabled me to accomplish this thesis successfully. Indeed His unlimited mercy and kindness remains my unremitting source of strength to face challenges in all fields of life. I would like to thank the School of Natural Sciences, National University of Sciences and Technology, Islamabad for their technical and academic support during my studies and research work. I am grateful to my supervisor Dr. Ibrar Hussain for his extended guidance and supervision. I am highly obliged and greatly indebted for his encouragement, continuous persuasion and facilitation throughout the research process. It would have been a very difficult task without his direction and guidance. I am obliged and owe a lot of thanks to my respectable guidance and examination committee members Prof Asghar Qadir, Dr. Mubasher Jamil and Dr. Sajid Ali. They were forthcoming in extending help and guidance at the time of need.

Finally, I appreciate the cooperation, support, encouragement and patience of my parents and siblings. Without them this work would never have come into existence (literally). Also special thanks to my sweet friend Lal Zaib Ali (for his support in good and bad time I have). This really facilitated in producing well throughout, focused and rationalized effort of this kind.

Tanveer Ahmad

Abstract

In this dissertation null and timelike geodesic motion in a slowly rotating Hořava-Lifshitz black hole are studied. First a review of null and timelike geodesics for radial and non-radial motion of particles in a static or non rotating Hořava-Lifshitz black hole is given. For this the behaviour of the effective potential is explained with the help of graphs. Then the timelike and null geodesic motion for radial and non-radial particle are studied for a slowly rotating Hořava-Lifshitz black hole. The behaviour of the effective potential for the particle is investigated and plotted. Especially our focus is on the spin parameter, a , of the black hole in Hořava-Lifshitz gravity. It is observed that in the case of the slowly rotating Hořava-Lifshitz black hole, the instability of the particle's effective potential increases by changing the values of angular momentum ℓ and the spin term a . There arise different cases due to energy of the motion of radial particle: (1) when the energy, E , of the particle is equal to E_C the critical energy (maximum value of the effective potential), then orbit of the particle becomes unstable; (2) if the energy, E , of the particle becomes greater than E_C , then the particle comes from infinity and fall into singularity; (3) when the energy, E , of the particle is less than E_1 , then orbit of the particle becomes stable, where E_1 , corresponds to the energy range, below which the motion of the particle goes into the bounded region.

Chapter 1

Introduction

General Relativity (GR) is a theory of gravitation. It explains several phenomena such as the bending of light due to gravity, gravitational redshift and perihelion shift of Mercury which is in complete agreement with the experimental facts [1]. However the limitations of the theory are felt at a microscopic level. For fundamental level the quantum description is required. There is no such theory that completely describes the motion of both microscopic and macroscopic objects. The problems also arise in dealing with the motion in which acceleration is due to fields other than gravity. This type of motion can be formally explained in the relativistic domain, but the argument is not in complete agreement with the philosophy of relativity [2].

GR is the only theory which explains the astrophysical and cosmological phenomena such as black hole, pulsars, quasars, density of stars, the big bang and the universe itself. It deals with the small shift (like perihelion shift) of the orbits of planets and it is also the essential ingredient in the system of global positioning system [3]. Einstein presented in 1915 the idea of space and geometry as a conceptual revolution of space and time in our views. Therefore in a gravitational field the falling of all objects with the same acceleration guided him to understand gravity in terms of curvature of spacetime. The presence of mass

induces curvature in the spacetime surrounding it. In the universe all bodies move along curved spacetime trajectories as a consequence of gravitation. The spacetime around the Sun becomes curved due to mass of the Sun and the planets move in the vicinity of curved trajectories in that spacetime. Gravity is geometry [4].

There are some relativistic phenomena and relativistic stars described below. Stars are stabilized by outward radiation pressure generated during nuclear reactions inside the star against the inward gravitational pull. In the star when nuclear fuel vanishes or is not enough, then gravitational attraction becomes dominant over the radiation pressure generated due to nuclear reaction within the star. Thus the gravitational collapse inside the star happens and core of the star becomes remarkably compact like “Neutron Stars” or “Black Holes” and “White Dwarfs” [5]. When the star’s mass $M \leq 1.44$ solar masses (Chandrasekhar limit) then this turns into a white dwarf. GR also put strict restriction on mass of the neutron up to the limit 3.2 solar mass [6] while crossing this limit leads to the formation of black hole. Moreover GR states that a black hole is formed when the gravitational pull on the surface becomes too large that it compacts the mass to the degree, such that nothing can escape through this surface, even light. According to Newton’s law of gravity an object with mass ‘ m ’ can escape from the vicinity of a star having mass ‘ M ’, with initial velocity greater than escape velocity ($v_{esc} = \sqrt{\frac{2GM}{R}}$). Therefore the object’s velocity exceeds from the velocity of light when $2GM > c^2R$. In Newtonian gravitational theory, there are no limitations for speed. It means that speed of an object can exceed the speed of light classically which is against the relativistic theory [7,9].

The black hole is described by its surface is known as event horizon. This means the boundary beyond which events cannot effect the outside observer. Objects may be captured in it but nothing can go out of it. Such objects was first proposed by Laplace and John Wheeler assign it with the name “black hole” [10]. For any star having mass ($M = 2 \times 10^{30}kg$), to convert into a black hole its radius would be about $0.3km$ [1].

Gravitational waves are also predicted by GR. As mass produces curvature in spacetime,

Thus the moving mass generates wavelets in spacetime that transmit with the speed of light. These wavelets are called gravitational waves. The gravitational waves sources are black holes, binary stars, big bang and supernova explosions. These waves cannot be detected easily due to weak gravitational pull. But due to these gravitational waves we are able to see the black hole horizon and other earlier events occurring in the universe more closely.

The dynamics of particle around a black hole is an important problem in black hole Astrophysics. This helps us in understanding the geometry of spacetime near the black hole. Motion of the particle might be predicted outside the black hole. In order to study these dynamics at quantum level, Hořava proposed a theory by using the concept of Lifshitz and named as Hořava-Lifshitz theory. It is a proposed theory of quantum gravity [11]. GR predicts that when an isolated spinning star collapses into black hole, gravitational radiations quickly remove any irregularity in rotation. Although, the typical spinning black hole is not isolated but it is surrounded by matter which is attracted to it. Moreover a rotating black hole may give enough energy to the particle that it gets escape to spatial infinity. This physical effect plays an important role in the ejection of high energy particles from accretion disks around the black hole [7].

Our main focus in this thesis is to find how a particle behaves when there associate a spin with slowly rotating black hole in HL gravity. We are interested in the effective potential's behaviour for the particle, that the instability of the particle increases or decreases by changing the values of angular momentum ℓ and spin parameter a .

To analyze the motion of a particle around a spinning black hole is a very complicated issue. Thus before dealing with a complicated problem of dynamics of a particle around a rotating black hole in HL gravity we start with a simpler case of static black hole in HL gravity. Generally the dynamical equations obtained through a Lagrangian or some other method for a particle, are not solvable analytically. In this thesis we assume the motion of particle in a slowly rotating HL black hole. The motion of a particle around a static black hole with no spin in HL gravity was studied by [12]. The main features of their study are, the effective

potential behavior for timelike geodesics motion of the particle and their radial motion in static black hole of HL gravity. Same problem for rotating case which have spin also, was studied by [13]. The main purpose is that if the rotating black hole have spin then it effects the effective potential. In this case, the action of spinning on the effective potential remains the same as in static black hole.

This dissertation has been divided into 4 chapters. The layout of the study is mentioned below:

1:- Chapter 1 covers the introduction and basic definitions

2:- Chapter 2 covers literature review of the motion of particle in a static black hole in the HL gravity.

3:- Chapter 3 covers the study about the motion of particle of slowly rotating black hole in the HL gravity.

4:- Chapter 4 covers results and conclusions.

We use the sign convention $(-, +, +, +)$ and units $c = 1$ and $G = 1$ through out this dissertation.

1.1 The Metric and Curvature Tensor

The position of a point in the spacetime can be determined by using its coordinates. But these coordinates do not give us complete information to explain their geometry in space. A metric tensor is a function which encode such information defined at each point in the space. It is a bilinear mapping of two vectors into real (\mathbb{R}), which means that it gives their inner product, shown as in [14]

$$\mathbf{g}(\vec{\mathbf{u}}, \vec{\mathbf{v}}) = \vec{\mathbf{u}} \cdot \vec{\mathbf{v}}. \quad (1.1.1)$$

The given definition suggests that the metric tensor is a symmetric tensor and their respective covariant and contravariant components are

$$g_{ab} = \mathbf{g}(\mathbf{e}_a, \mathbf{e}_b) = \mathbf{e}_a \cdot \mathbf{e}_b \quad (1.1.2)$$

$$g^{ab} = \mathbf{g}(\mathbf{e}^a, \mathbf{e}^b) = \mathbf{e}^a \cdot \mathbf{e}^b. \quad (1.1.3)$$

Here g_{ab} is a non singular covariant metric tensor. Where non-singular means that its determinant is non-zero in terms of its components. It is a covariant symmetric $g_{ab} = g_{ba}$ tensor-field of rank 2. There exists a unique inverse represented by g^{ab} which guarantees that the rank of the inverse metric is also 2.

The metric tensor is used to define the infinitesimal distance ds , between two points on a curve $x^a(p)$ and $x^a(p + \Delta p)$. Let V be the tangent vector field of the curve then

$$ds^2 = g(\mathbf{v}, \mathbf{v})dp^2 = g_{ab}v^av^bdp^2 = g_{ab}dx^adx^b, \quad (1.1.4)$$

here $v^a = \frac{dx^i}{dp}$. The quantity ds^2 is known as the line element associated with the metric tensor g_{ab} . It is now assumed to be a function of several variables. A function may be multi-linear if it is linear in all of its arguments. Thus a tensor is a multi-linear function that maps vectors and one form into \mathbb{R} .

Riemann Curvature Tensor

The Riemann curvature tensor plays an important role in describing the geometrical properties of spacetime. It explains the curvature in an invariant way. Let us consider a covariant derivative of a tensor of rank one [1]

$$X^a{}_{;c} = X^a{}_{,c} + \Gamma^a{}_{bc}X^b. \quad (1.1.5)$$

Taking again the derivative we obtain

$$(X^a{}_{;c})_{;d} = (X^a{}_{,c})_{,d} + \Gamma^a{}_{ed}(X^e{}_{;c}) - \Gamma^e{}_{cd}(X^a{}_{;e}), \quad (1.1.6)$$

expanding this equation which gives

$$X^a{}_{;c;d} = (X^a{}_{,c} + \Gamma^a{}_{bc}X^b)_{,d} + \Gamma^a{}_{ed}(X^e{}_{,c} + \Gamma^e{}_{bc}X^b) - \Gamma^e{}_{cd}(X^a{}_{,e} + \Gamma^a{}_{be}X^b). \quad (1.1.7)$$

Now following the same procedure but with change in order of the derivatives implies that

$$X^a{}_{;d;c} = (X^a{}_{,d} + \Gamma^a{}_{bd}X^b)_{,c} + \Gamma^a{}_{ec}(X^e{}_{,d} + \Gamma^e{}_{bd}X^b) - \Gamma^e{}_{dc}(X^a{}_{,e} + \Gamma^a{}_{be}X^b). \quad (1.1.8)$$

Subtracting equation (1.1.7) from equation (1.1.8) and comparing their dummy indices gives

$$X^a{}_{;d;c} - X^a{}_{;c;d} = R^a{}_{bcd}X^b + (\Gamma^e{}_{cd} - \Gamma^e{}_{dc})\nabla_e X^a, \quad (1.1.9)$$

where as

$$R^a{}_{bcd} = \Gamma^a{}_{bd,c} - \Gamma^a{}_{bc,d} + \Gamma^e{}_{bd}\Gamma^a{}_{ec} - \Gamma^e{}_{bc}\Gamma^a{}_{ed}, \quad (1.1.10)$$

while $\Gamma^e{}_{cd} = \Gamma^e{}_{dc}$, then equation (1.1.9) reduces to

$$X^a{}_{;d;c} - X^a{}_{;c;d} = R^a{}_{bcd}X^b. \quad (1.1.11)$$

Thus $R^a{}_{bcd}$ is called Riemann tensor and it describes the curvature of space. If $R^a{}_{bcd} = 0$, then the given space is flat while if $R^a{}_{bcd} \neq 0$, then the space is curved. The Riemann curvature tensor can also be written as

$$R_{abcd} = g_{ae}R^e{}_{bcd}. \quad (1.1.12)$$

Here R_{abcd} is skew symmetric in the first two indices and last two indices

$$R_{abcd} = R_{bacd}, \quad R_{abcd} = R_{abdc}. \quad (1.1.13)$$

R_{abcd} is symmetric with respect to the pair of the indices under permutation

$$R_{abcd} = R_{cdab}, \quad (1.1.14)$$

and R_{abcd} satisfies the following two Bianchi identities

$$R^a{}_{bcd} + R^a{}_{cdb} + R^a{}_{dbc} = 0, \quad (1.1.15)$$

$$R_{abcd;e} + R_{abde;c} + R_{abec;d} = 0. \quad (1.1.16)$$

Here semicolon “;” in the given expression represents the covariant derivative. The Riemann curvature tensor (1.1.12) have n^4 independent components while using properties (1.1.13) to (1.1.15) these components reduces to $\frac{n^2(n^2-1)}{12}$ [14].

The Ricci Tensor: This is simply a trace of R_{abcd} . From equation (1.1.12) applying contraction on first and third indices respectively we get [4]

$$R_{bd} = R^a{}_{bad}. \quad (1.1.17)$$

This is a symmetric tensor with rank 2 which is known as Ricci tensor.

The Ricci Scalar: By contracting R_{ab} with g^{ab} it gives curvature scalar (Ricci scalar) R [4],

$$R = g^{ab}R_{ab}. \quad (1.1.18)$$

This Ricci scalar is the trace of Ricci tensor.

The Einstein Tensor: To derive the Einstein tensor we are using Bianchi identity as follow

$$R_{abcd;e} + R_{abde;c} + R_{abec;d} = 0. \quad (1.1.19)$$

Raising the first index 'a' and then contract it with index d implies that

$$R_{bc;e} + R^a{}_{bae;c} + R^a{}_{bec;a} = 0. \quad (1.1.20)$$

Applying the antisymmetric property on second term yields

$$R_{bc;e} + R_{be;c} + R^a{}_{bec;a} = 0. \quad (1.1.21)$$

Raise the index b and then contract it with e we obtain

$$R^b{}_{c;b} - R_{;c} + R^{ab}{}_{bc;a} = 0. \quad (1.1.22)$$

By using the symmetry property we get

$$R^{ab}{}_{bc;a} = R^{ba}{}_{cb;a} = R^a{}_{c;a} = R^b{}_{b;c}. \quad (1.1.23)$$

Thus the first and last terms are same in equation (1.1.22) which becomes

$$2R^b{}_{c;b} - R_{;c} = 0. \quad (1.1.24)$$

Where

$$(2R^b{}_c - \delta^b{}_c R)_{;b} = 0. \quad (1.1.25)$$

By raising the index c we obtain the Einstein tensor

$$(R^{bc} - \frac{1}{2}g^{bc}R)_{;b} = 0. \quad (1.1.26)$$

The inner expression in the parenthesis called Einstein tensor usually represented by

$$G^{ab} \equiv R^{ab} - \frac{1}{2}g^{ab}R. \quad (1.1.27)$$

The Einstein tensor is divergence free and symmetric. This is the tensor which describes the geometric behavior of spacetime in the field equations of GR.

1.2 The Einstein Field Equations

Now this is the exact time to derive the Einstein field equations (EFE's). We start from the variational principle,

$$\delta S_G = 0, \quad (1.2.1)$$

here S_G is the gravitational action [14]. It is geometrical so its Lagrangian is

$$S_G = \frac{1}{2\kappa} \int_M \mathcal{L}_G(g_{ab}, g_{ab,c}) \sqrt{-g} d^4x. \quad (1.2.2)$$

Here $\kappa = 8\pi$ is a constant and can be calculated according to the required condition. In the weak field limit the EFE's reduces into Newton's law. Also the Lagrangian for the field is as under

$$\mathcal{L}_G(g_{ab}, g_{ab,c}) = R - 2\Lambda, \quad (1.2.3)$$

here Λ is the cosmological constant. Substitute this value in equation (1.2.2) which becomes

$$S_G = \frac{1}{2\kappa} \int (R - 2\Lambda) \sqrt{-g} d^4x = \frac{1}{2\kappa} \int (g^{ab} \sqrt{-g} R_{ab} - 2\Lambda \sqrt{-g}) d^4x, \quad (1.2.4)$$

where

$$\delta S_G = \frac{1}{2\kappa} \int (g^{ab} \sqrt{-g} \delta R_{ab} + R_{ab} \delta g^{ab} \sqrt{-g} - 2\Lambda \delta \sqrt{-g}) d^4x. \quad (1.2.5)$$

We consider here a small volume element V with supposition that two conditions are satisfied on its boundary i.e. variation of the metric and its first derivative becomes zero. Now to introduce local coordinate system in this region V , we have $\Gamma^a_{bd} = 0$ then Ricci tensor is given by equation (1.1.10) becomes

$$R_{ab} = \Gamma^c_{ab,c} - \Gamma^c_{ac,b}. \quad (1.2.6)$$

Thus

$$\delta R_{ab} = \delta \Gamma^c_{ab,c} - \delta \Gamma^c_{ac,b}. \quad (1.2.7)$$

While the partial derivative also commute with the variation and it vanishes at the boundary of V . Then the above expression becomes

$$g^{ab} \delta R_{ab} = (g^{ab} \delta \Gamma^c_{ab} - g^{ac} \delta \Gamma^b_{ab})_{,c}. \quad (1.2.8)$$

By introducing a vector X^c we have

$$X^c = g^{ab}\delta\Gamma^c_{ab} - g^{ac}\delta\Gamma^b_{ab}. \quad (1.2.9)$$

Replacing this in equation (1.2.8) it can be written as

$$g^{ab}\delta R_{ab} = X^a_{,a}, \quad (1.2.10)$$

this is the total divergence. As said earlier that metric tensor and its differentiation becomes zero at the boundaries. From stoke's theorem the first term will disappear and have no contribution in δS_G

$$\int (\sqrt{-g}g^{ab}\delta R_{ab})d^4x = 0. \quad (1.2.11)$$

While

$$\delta\sqrt{-g} = \left[\frac{\partial\sqrt{-g}}{\partial g_{cd}} \right] \delta g_{cd} = -\frac{1}{2\sqrt{-g}} \left(\frac{\partial g}{\partial g_{cd}} \right) \delta g_{cd} \quad (1.2.12)$$

$$\delta\sqrt{-g} = \frac{1}{2}\sqrt{-g}g^{cd}\delta g_{cd}. \quad (1.2.13)$$

Now the second term becomes

$$\delta[g^{ab}\sqrt{-g}] = \sqrt{-g}\delta g^{ab} + g^{ab}\delta\sqrt{-g}. \quad (1.2.14)$$

Since we know that $g^{ac}g_{cd} = \delta^a_d$. We obtain

$$\delta(g^{ac}g_{cd}) = 0. \quad (1.2.15)$$

Thus it can be written as

$$\delta g_{cd} = -g_{ac}g_{bd}\delta g^{ab}. \quad (1.2.16)$$

After substituting this value in equation (1.2.13) and then re arranging we get

$$\delta[g^{ab}\sqrt{-g}] = \sqrt{-g}(\delta g^{ab} - \frac{1}{2}g^{ab}g_{cd}\delta g^{cd}). \quad (1.2.17)$$

Now put value from equation (1.2.13) and equation (1.2.17) in equation (1.2.5) which leads

$$\delta S_G = \frac{1}{2\kappa} \int \sqrt{-g}(R_{cd} - \frac{1}{2}Rg_{cd} + \Lambda g_{cd})\delta g^{cd}d^4x. \quad (1.2.18)$$

In general theory of relativity the vacuum field equations require that the $\delta S_G = 0$, for any arbitrary variation in the metric explained by [14]. If the integrand is zero then the variation in action δS_G can be zero. Thus we obtain from the above equation (1.1.10)

$$R_{cd} - \frac{1}{2}Rg_{cd} + \Lambda g_{cd} = 0. \quad (1.2.19)$$

This is the required vacuum field equations. Here g_{cd} and R_{cd} are symmetric. Therefore there are only ten field equations and having ten independent components.

The Einstein Field Equations in the Presence of Matter

In order to obtain the full version of EFE's, we consider that there exists other fields rather than gravitational field. These fields can be explained in terms of Lagrangian density \mathcal{L}_M , where the action is given by [1],

$$S = \frac{1}{2\kappa} \int (\mathcal{L}_G + \mathcal{L}_M) \sqrt{-g} d^4x = \frac{1}{2\kappa} \int \mathcal{L}_G \sqrt{-g} d^4x + \frac{1}{2\kappa} \int \mathcal{L}_M \sqrt{-g} d^4x. \quad (1.2.20)$$

This implies that

$$S = (S_G + S_M). \quad (1.2.21)$$

According to the variational principle

$$\delta S = \delta(S_G + S_M) = 0. \quad (1.2.22)$$

The action integral for matter and energy is

$$S_M = \int \mathcal{L}_M(g_{ab}, g_{ab,c}) \sqrt{-g} d^4x. \quad (1.2.23)$$

For variation in argument gives

$$\delta[\sqrt{-g}\mathcal{L}_M(g_{ab}, g_{ab,c})] = \frac{\partial[\sqrt{-g}\mathcal{L}_M]}{\partial g^{ab}} \delta g^{ab} + \frac{\partial[\sqrt{-g}\mathcal{L}_M]}{\partial g^{ab}_{,c}} \delta g^{ab}_{,c}. \quad (1.2.24)$$

By introducing a vector X^c as

$$X^c = \frac{\partial[\sqrt{-g}\mathcal{L}_M]}{\partial g^{ab}_{,c}} \delta g^{ab}. \quad (1.2.25)$$

The divergence of vector X^c is

$$X^c{}_{,c} = \left[\frac{\partial[\sqrt{-g}\mathcal{L}_M]}{\partial g^{ab}{}_{,c}} \right]_{,c} \delta g^{ab} + \frac{\partial[\sqrt{-g}\mathcal{L}_M]}{\partial g^{ab}{}_{,c}} \delta g^{ab}{}_{,c}. \quad (1.2.26)$$

From equation (1.2.24) and equation (1.2.26)

$$\delta[\sqrt{-g}\mathcal{L}_M] = \frac{\partial[\sqrt{-g}\mathcal{L}_M]}{\partial g^{ab}} \delta g^{ab} - \left[\frac{\partial[\sqrt{-g}\mathcal{L}_M]}{\partial g^{ab}{}_{,c}} \right]_{,c} \delta g^{ab} + X^c{}_{,c}. \quad (1.2.27)$$

As we supposed that the variation becomes zero at the boundary, so the integral $\int X^c{}_{,c} d^4x = 0$. This concludes

$$\delta S_M = \int \left(\frac{\partial[\sqrt{-g}\mathcal{L}_M]}{\partial g^{ab}} - \left[\frac{\partial[\sqrt{-g}\mathcal{L}_M]}{\partial g^{ab}{}_{,c}} \right]_{,c} \right) \delta g^{ab} d^4x. \quad (1.2.28)$$

Here the energy momentum tensor \mathcal{L}_M is defined as

$$T_{ab} = -\frac{2}{\sqrt{-g}} \left(\frac{\partial[\sqrt{-g}\mathcal{L}_M]}{\partial g^{ab}} - \left[\frac{\partial[\sqrt{-g}\mathcal{L}_M]}{\partial g^{ab}{}_{,c}} \right]_{,c} \right). \quad (1.2.29)$$

simplifying this we arrive

$$\delta S_M = -\frac{1}{2} \int T_{ab} \sqrt{-g} \delta g^{ab} d^4x. \quad (1.2.30)$$

From equation (1.2.18) and (1.2.30) we obtain the gravitational field equation in the presence of matter and energy.

$$R_{ab} - \frac{1}{2} R g_{ab} + \Lambda g_{ab} = \kappa T_{ab}. \quad (1.2.31)$$

These are the required Einstein field equations. The stress energy tensor is divergence free like Einstein tensor and this also assures the conservation of energy and momentum.

1.3 Notation and Terminology

Spacetime

The physical 4-dimensional manifold which has three spatial coordinates and one temporal coordinate is called spacetime, in which all physical quantities can be located.

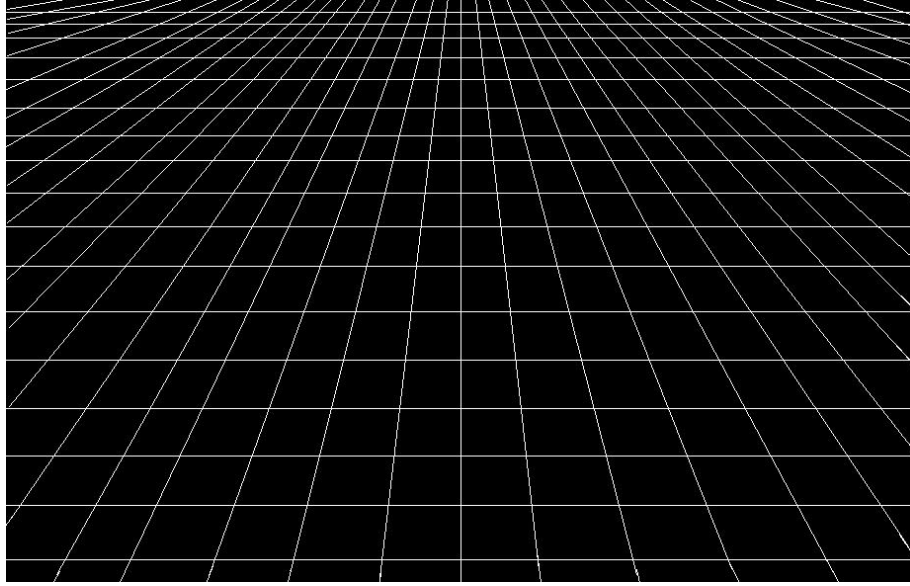


Figure 1.1: Flat Space-time, Courtesy: Google

Asymptotically flat spacetime:- When the geometry of a spacetime becomes flat at large distances from its sources in the gravitational field. Then it is known as an asymptotically flat spacetimes [15]. For flat spacetime the the Riemann curvature tensor becomes zero, i.e. $R^a_{bcd} = 0$. Its metric can be read as

$$ds^2 = -dt^2 + dr^2 = \eta_{ab}dx^a dx^b. \quad (1.3.1)$$

Here $\eta_{\alpha\beta} = \text{diag}[-1, 1, 1, 1]$ often represents flat spacetime metric [15].

Curved Space-time:- Einstein's geometric theory of gravitation, incorporating and expanding the special relativity to the accelerated frame of reference and by introducing the principle that gravity is the consequence of matter that causes curvature in spacetime. Riemann curvature tensor is non-zero i.e. $R^a_{bcd} \neq 0$, for curved spacetimes.

Spherical Symmetry:- Spherical symmetry means that every point will lie on same surface of the sphere. It means that one can go from one point to another on the sphere by means of a rotation. Simply if an object is rotated through any axis it gets the same shape. This is called spherical symmetry [16].

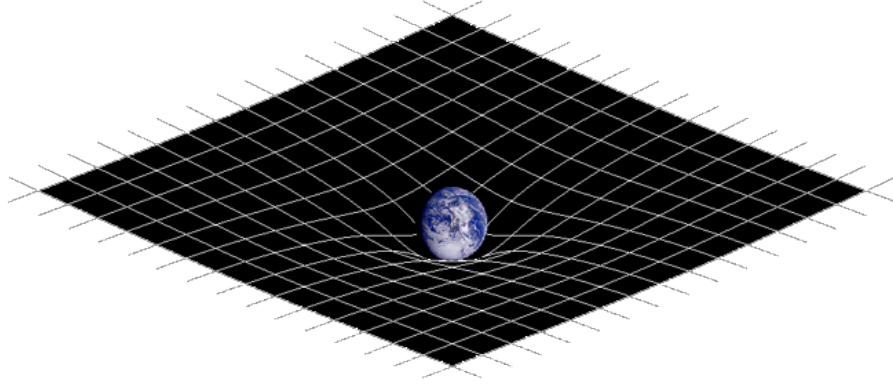


Figure 1.2: Curved Space-time, Courtesy: Google

Event Horizon

It is a partition in spacetime beyond which events have no affect on an outside observer. Event horizon is the boundary between its inside and outside of the black hole spacetime. It means that the outside observer does not know anything about events happening inside .

Spacetime Singularity

The spacetime singularity or gravitational singularity is a point (location) where the quantities used for the measurement of gravitational field becomes infinite in such a way that does not depend on coordinate system. For example in Schwarzschild metric which is given as [17]

$$ds^2 = -\left(1 - \frac{2M}{r}\right)dt^2 + \frac{1}{\left(1 - \frac{2M}{r}\right)}dr^2 + r^2d\Omega^2. \quad (1.3.2)$$

It can be shown that at $r = r_s$ and $r = 0$, the metric become singular. Here $d\Omega^2 = (d\theta^2 + \sin^2\theta d\phi^2)$ and r_s is the Schwarzschild radius which is equal to $r_s = 2M$. Thus at $r = r_s$, the coefficient of dr^2 tends to infinity while at $r = 0$, the coefficient of dt^2 approaches to infinity [12]. There are three types of singularities which is given as:

(1) **Physical Singularity**:- It is the location where the curvature becomes infinitely large [17]. In equation (1.3.3) at $r = 0$ the singularity becomes physical singularity and the curvature approaches to infinity.

(2) **Coordinate Singularity** :- It is a surface (location) where only one component of the metric tensor becomes infinitely large, while the spacetime curvature is finite [18].

(3) **Naked Singularity**:- That gravitational singularity which has no event horizon, simply means without any boundary.

Doppler Redshift

This term explains the condition that when an astronomical body is observed to move away from the observer, the light emitted by the body which is going away is increased in wavelength and it shifted to the red region of the spectrum. We represents this by $z = \frac{(\lambda - \lambda_0)}{\lambda_0}$, where λ_0 is the emitted wavelength while λ is the observed wavelength of the radiation.

Gravitational Redshift:- The frequency of the photon shifts to the lower energy when the photon jumps out of the gravitational field. It is called gravitational redshift [18]. The photon red shift z is defined as

$$1 + z = \left(\frac{\nu_R}{\nu_E} \right)^{-1}. \quad (1.3.3)$$

Where ν_E is the frequency of the emitter and ν_R represents the frequency of the receiver.

Effective Potential

It is a mathematical equation that combines both effects attractive and repulsive in a single potential energy of a dynamical system. The effective potential contains both positive as well as negative term in its mathematical expression. e.g

$$V_{eff}^2 = \left(1 - \frac{2M}{r} \right) \left(1 + \frac{L^2}{r^2} \right). \quad (1.3.4)$$

Orbit

It represents a closed path for an object rotating around a central body like a star or a black hole, under the influence of gravitational field. There are two types of orbits, stable orbit and unstable orbit.

Stable Orbit:- The minimum value of the effective potential for black holes corresponds to

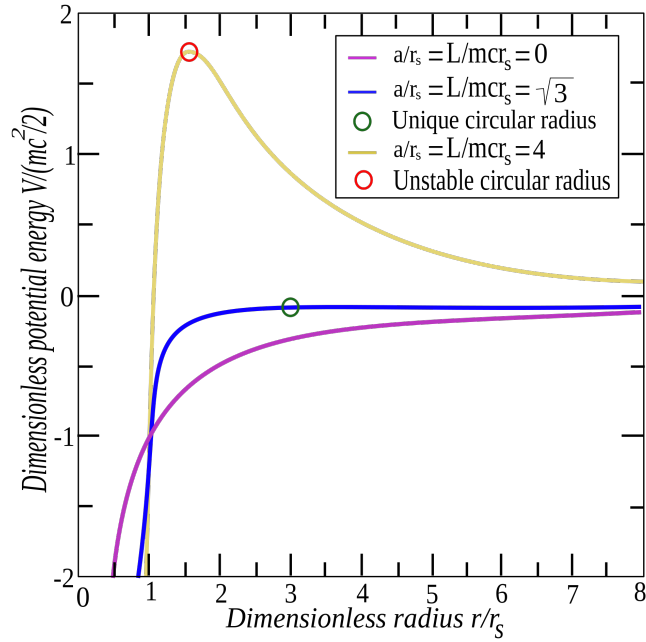


Figure 1.3: Stable and Unstable Orbits Graph [7]

the stable orbit. In fig (1.3) the circle on blue line represents the unique circular radius. For stable circular orbits it is necessary to hold these conditions $V'|_{r_0} = 0$ and $V''|_{r_0} > 0$ [19], where r_0 is the coordinate distance of the particle's closest approach to the black hole [7].

Unstable Orbit:- The maximum value of the effective potential for black holes corresponds to the unstable orbit of the radial motion of the particle as described in the Figure (1.3). Here the red circle denotes the unstable circular radius. For unstable orbit the conditions are $V'|_{r_0} = 0$ and $V''|_{r_0} < 0$

1.4 Black Holes

Black holes come as a result of the solution of EFE's. In fact these are the singular solutions of the EFE's. A black hole is a place where gravity becomes too much strong that the escape velocity is greater than that of light. The birth of a black hole takes place from death of a

super massive star. A complete description is as under [17]:

The star defends itself against two types of forces, gravitational pull and pushing of the pressure in outward direction. Enough amount of pressure and energy is produced due to thermonuclear reactions in stars. In general situations in stars, there is a tug of war game between gravity and pressure. As far as these two forces (gravity and pressure) balances each other, then star will remain stable. However, when the nuclear fuel exhausts, as a result the thermonuclear pressure comes to decrease and the balance between gravity and pressure disturbs. The star begins to contract when the star becomes massive. The more massive the star, the more will be its gravity, so gravity gets an upper hand of all the outward forces and star starts collapsing. The volume of the star gets smaller and smaller while density of the star increases time by time. The escape velocity within such a packed surface exceeds the velocity of light, and then the star becomes a black hole.

In case of small stars, when the nuclear fuel in the star gets finished and there is no further response to gravity and the electronic repulsive force in star creates more gravitational collapse, thus the star becomes cool and vanishes silently, such stars are called “White Dwarf” [19].

1.4.1 History of Black Holes

Black holes are one of the most mysterious thing in the scientific world. The concept of a super-dense matter’s sphere that even light can not escape through it, is somewhat incredible even today. Through this topic it will be tried to flash some light on these strange formations, and tell about the most accepted and popular theories of scientists as follow:

In 1784 an English geologist **John Mitchell** started work on Newton’s gravitational theory. According to Newtonian Physics that a ball strike by the cannon will rotate around the earth in orbits. The velocity of the ball increases and reaches to particular range called escape velocity of the planet. This escape velocity depends on mass and radius of the object.

Mitchell emphasized that a star which is much massive and compact have such a strong gravitational field that even light can't escape from it: light emitted from the star's surface would be pulled back by the star's gravitational field [20]. Mitchell suggested that there might exists a large number of such stars. Although we cannot see them because light cannot reach us from these stars, but still we feel their gravitational attraction.

A few year later similar suggestion was made by a French mathematician **Marquis de Laplace**. In 1796 he said that in fact it is not true to manage light like cannon balls in Newton's gravitational theory because speed of light is constant. A regular theory about gravity affects the light did not come until Einstein's GR theory [16]. Albert Einstein was a German physicist, he struggled a lot with his equations to solve but can not get success. At last in 1915 he published his first paper on GR. Black holes are predicted by GR, but even himself Einstein did not believe that they exist. The general invariance principle is a dynamical principle that forces limitations on possible interactions of geometry and matter [19]. **Karl Schwarzschild** a German physicist one year later, in 1916 found a solution to the EFE's. The Schwarzschild's solution is for non rotating stationary black holes. If a star converted to a black hole then there exists a horizon at Schwarzschild radius [14].

In 1930 an Indian-American physicist **Subrahmanyan Chandrasekhar** found that for stellar mass $M = 1.4M_{\odot}$ (M_{\odot} denotes solar mass), the repulsive force (electron degenerate pressure) will not be so strong to dominate the gravitational contraction. Stars mass come under this limit will resist the gravitational collapse by the electron's fermionic repulsion becomes white dwarf [19].

In 1939 an American Physicist **Julius Robert Oppenheimer** and **Hartland Synder** founded that in essence, black holes could be formed in nature by the collapse of some heavy objects (Stars) [20]. In 1963 **Roy Kerr** presented a theoretical explanation of spinning black holes [21].

In 1967 an American Physicist named **John Archibald Wheeler** used the word "black

hole” in the theory for the first time. According to Wheeler black holes are simply described by three parameters to specify its picture completely. (1) mass (2) angular momentum (specifying their rotation) and (3) electric charge.

In 1974 the British theoretical physicist **Stephen Hawking** come across that quantum black holes are not too black as like classical ones. Hawking gave the derivation of black holes radiations. His results have no direct connection to quantum gravity [22].

1.5 Hořava-Lifshitz Gravity

Quantum Gravity (QG) is the theory that seeks to explain gravity according to the principles of quantum mechanics. The current gravity is based on Einstein’s theory of GR, which is formulated classically. To solve the problems arising at quantum level in GR there is a need to make a connection between GR and quantum mechanics. Therefore different theories were proposed at different times. Peter Hořava suggested a theory of QG in 2009 which is named Hořava-Lifshitz gravity or HL gravity theory where its action is [23]

$$S_g = \int dt d^3x \sqrt{g} N (\mathcal{L}_k + \mathcal{L}_v). \quad (1.5.1)$$

In this equation the kinetic term is given by

$$\mathcal{L}_k = \frac{2}{\kappa^2} (K_{ab} K^{ab} - \lambda K^2), \quad (1.5.2)$$

where the extrinsic curvature becomes

$$K_{ab} = \frac{1}{2N} (\dot{g}_{ab} - \nabla_a N_b - \nabla_b N_a). \quad (1.5.3)$$

The potential term in the equation is given by

$$\mathcal{L}_v = -\frac{\kappa^2}{8} E^{ab} G_{ab,cd} E^{cd}, \quad (1.5.4)$$

here the super-metric $G_{ab,cd}$ depends upon a dimensionless arbitrary coupling constant ‘ λ ’, where

$$G_{ab,cd} = \frac{1}{2} (g_{ac} g_{bd} + g_{ad} g_{bc}) + \frac{\lambda}{1 - 3\lambda} g_{ab} g_{cd}. \quad (1.5.5)$$

The tensor E is given as

$$E^{ab} = \frac{2}{\omega^2} C^{ab} - \mu \left(R^{ab} - \frac{1}{2} R g^{ab} + \Lambda_\omega g^{ab} \right), \quad (1.5.6)$$

where

$$C^{ab} = \frac{\epsilon^{acd}}{\sqrt{g}} \nabla_c \left(R^b{}_d - \frac{1}{4} R \delta^b{}_d \right). \quad (1.5.7)$$

Here $\kappa = [Mass]^{-1}$, $\omega = [Mass]^0$ and $\mu = [Mass]^1$ are constants and Λ_ω is a cosmological constant. This theory provides solution to different issues of time in quantum field theory and GR where quantum concept serves as the more fundamental. HL gravity has the 4-dimensional spacetime in QG. That clearly violates the local Lorentz invariance. QG is a power counting renormalizable theory. At large distances it reduces to Einstein GR. This theory provides an ultraviolet completion of GR [21]. In the HL gravity theory the static and rotating black holes solutions are being studied in recent years. It is a fascinating QG theory, which has progressive and restoring study on cosmology and black holes solutions [23,24]. In HL gravity it is expected that the black hole solutions asymptotically become Einstein gravity solutions e.g. the Kehagias-Sfetsos (KS) solution (will be discussed in the next section) is one of them [25].

1.6 Black Holes in Hořava-Lifshitz Gravity

The HL gravity theory has a refreshing and advanced work on black hole solutions and cosmology. This theory provides solutions to black holes. One of the black hole solutions in HL gravity was obtained by Lu-Mei-Pope (LMP) [26]. This solution is spherically symmetric with some dynamic parameter ' λ '. An asymptotically flat black hole solution was found by Kehagias and Sfetsos, using deformed HL gravity [27] and parameter $\lambda = 1$. Line element for these black holes is

$$ds^2 = -f(r)dt^2 + \frac{dr^2}{f(r)} + r^2(d\theta^2 + \sin^2\theta d\phi^2), \quad (1.6.1)$$

where lapse function i.e. $f(r)$, for LMP solution is

$$f_{LMP} = 1 - \Lambda_w r^2 - \frac{\alpha}{\sqrt{-\Lambda_w}} \sqrt{r}, \quad (1.6.2)$$

and lapse function $f(r)$, for the KS solution is

$$f_{KS}(r) = 1 + \omega r^2 - \sqrt{r(\omega^2 r^3 + 4\omega M)}. \quad (1.6.3)$$

HL gravity also provides solution to the slowly rotating black holes [28]. Slowly rotating means that the rotating parameter ($a = \frac{J}{M}$) is considered up to linear order in equations of motion and in the metric functions. General line element for a slowly rotating black hole is given by [29]

$$ds^2 = -f(r)dt^2 + \frac{dr^2}{f(r)} + r^2 d\theta^2 + r^2 \sin^2 \theta [d\phi^2 - 2aN^\phi(r)dt d\phi]. \quad (1.6.4)$$

In this line element $f(r)$ represents the lapse function as given by the equation (1.6.3), while $N^\phi(r)$ is called the shift function and it is $N^\phi(r) = \frac{2M}{r^3}$.

1.7 Particle Dynamics in Black Hole Space-times

The motion of a small particle in the presence of external forces is known as particle dynamics, e.g. in the presence of gravitational force and electromagnetic force. Science of mechanics searches to provide a consistent and precise explanation for the dynamics of particles and systems of particles.

In GR particle dynamics around black hole remained subject of interest for physicists for the last many years. In this regard many people worked on this subject e.g motion of particle in the background geometry of Kerr spacetime [30], where W. Han investigated the relation between orbits chaos and spin magnitudes S , polar angle and Kerr rotation parameter ‘ a ’ through brand new Fast Lyapunov Indicator (FLI). Motion of the particle in Kerr, Kerr-Newmann (KN) and Reissner-Nordström (RN) was studied by Pugliese et al [31-34]. They

found the dynamics of neutral test particle in the gravitational field of mass M with a charge Q . They concentrated on the study of circular stable and unstable orbits around system expressing either naked singularities or black holes. Due to existence of repulsive gravity, they showed that at classical radius described by $\frac{Q^2}{M}$, there exists zero angular momentum orbits. The stability of circular orbits analysis indicates that black holes are defined by a continuous region of stability. They also showed the geometry of stable accretion disk, made by test particles only, moving along circular orbits around central body allows to distinguish clearly between black holes and naked singularities. Furthermore they found that the gravitational acceleration is repulsive in area of the inception of RN and Kerr spacetimes and at large distances it becomes attractive in the expected Newtonian way. In regular black hole spacetime, dynamics was studied by Garcia et. al [35]. They discussed the entire set of orbits for neutral and weakly charged particles, containing for extreme metric. Garcia et. al also derived the analytical solutions to the equation of motion for neutral test particle in a parametric form. Similarly it is also important to study these particle dynamics in HL gravity. Motion of particle around KS black hole immersed in an external magnetic field was investigated in [36]. In that paper they studied the strong dependence of the removed energy from special range of the parameters of the HL gravity, where parameters are Λ_w and specific angular parameter a . Abdujabbarov discussed the particle acceleration near the rotating black hole in HL gravity. It is manifest that the fundamental parameter of HL gravity can impose a limitation on the energy of accelerating particles to restrict them from infinite value. In [37] charged particles motion in a rotating black hole immersed in uniform magnetic field has studied. Particle dynamics are also discussed in [13]. In that paper they calculated the center of mass energy of two colliding particles near the static and rotating HL black holes. They compare their results of HL black hole with that of the Kerr black holes. From their study they confirmed the finite value of center of mass energy for static and infinite value of center of mass energy for rotating black holes. They studied that the center of mass energy depends on temperature of the black hole horizon. From that they obtained the critical angular momentum for the particles. They also showed that the energy of the center of mass of two colliding particles in the vicinity of the rotating HL black hole could be

arbitrarily high. In [12] J. Chen and Y. Wang analyzed the behaviour of effective potential for the particle to investigate the timelike geodesic motion of the particle in HL spacetime. Motion of particle in the background geometry of magnetized schwarzschild black hole has also been discussed in [38]. M. Jamil et. al analyzed the motion of a charged and neutral particle around a spherically symmetric and static black hole, in the existence of quintessence matter and external magnetic field. They inspected the conditions for particle around black hole when it escape to infinity after the collision with another particle. They discussed in detail the inner most stable circular orbit (ISCO) for the particle and its dependence on dark energy, and also on the external magnetic field around the black hole. By using Lyapunov exponent they compared the stabilities of particles orbits in the presence and absence of dark energy and magnetic field. They derived the expressions for center of mass energies for the colliding particles near the black hole horizon.

1.8 Geodesic Equations

Geodesic represents the shortest path between two points in curved spacetime geometry. There are two types of geodesics.

Timelike Geodesic:- It is defined as the maximum/minimum distance between two points on the curve and it lies within the light cone [20].

Null Geodesic:- The infinitesimal distance between two points on the curve is equal to zero is known as null geodesics. It is the path of the light like particles or photons. It represents the light cone. Geodesics equations are derived below.

The geodesic Lagrangian for a particle of unit mass is

$$\mathcal{L} = \frac{1}{2}g_{cd}\dot{x}^c\dot{x}^d, \quad (1.8.1)$$

where $g_{cd} = g_{cd}(x^e)$. Now the Euler-Lagrange equations are written in the form

$$\frac{d}{d\tau} \left(\frac{\partial \mathcal{L}}{\partial \dot{x}^b} \right) - \frac{\partial \mathcal{L}}{\partial x^b} = 0. \quad (1.8.2)$$

From equation (1.8.1)

$$\left(\frac{\partial \mathcal{L}}{\partial \dot{x}^b}\right) = g_{bd}\dot{x}^d, \quad (1.8.3)$$

and

$$\frac{\partial \mathcal{L}}{\partial x^b} = \frac{1}{2}g_{cd,b}\dot{x}^c\dot{x}^d. \quad (1.8.4)$$

Differentiating equation (1.8.3) w.r.t ‘ τ ’, we have

$$\frac{d}{d\tau}\left(\frac{\partial \mathcal{L}}{\partial \dot{x}^b}\right) = g_{bd,c}\dot{x}^c\dot{x}^d + g_{bd}\ddot{x}^d. \quad (1.8.5)$$

Using equation (1.8.4) and equation (1.8.5) in equation (1.8.2), we obtain

$$g_{bd,c}\dot{x}^c\dot{x}^d + g_{bd}\ddot{x}^d - \frac{1}{2}g_{cd,b}\dot{x}^c\dot{x}^d = 0, \quad (1.8.6)$$

where we have

$$g_{bd,c}\dot{x}^c\dot{x}^d = \frac{1}{2}(g_{bd,c} + g_{bc,d})\dot{x}^c\dot{x}^d. \quad (1.8.7)$$

Using equation (1.8.7) in equation (1.8.6), we get

$$g_{bd}\ddot{x}^d + \frac{1}{2}(g_{bc,d} + g_{bd,c} - g_{cd,b})\dot{x}^b\dot{x}^d = 0. \quad (1.8.8)$$

Multiplying g^{ab} on both sides of equation (1.8.8), we arrive at

$$g^{ab}[g_{bd}\ddot{x}^d + \frac{1}{2}(g_{bd,c} + g_{bc,d} - g_{cd,b})\dot{x}^b\dot{x}^d] = 0. \quad (1.8.9)$$

This gives the geodesics equation of motion [22]

$$\ddot{x}^a + \Gamma_{cd}^a\dot{x}^c\dot{x}^d = 0, \quad (1.8.10)$$

where Γ_{cd}^a , is the Christoffel symbol and is defined by

$$\Gamma_{cd}^a = \frac{1}{2}g^{ab}(g_{bd,c} + g_{bc,d} - g_{cd,b}). \quad (1.8.11)$$

Chapter 2

Motion of a Particle in the Vicinity of Static Hořava-Lifshitz Black Holes

In this chapter the motion of a particle in static HL black holes will be reviewed. Here we will review timelike geodesic motion of a particle in the back ground geometry of a static black hole in HL gravity. This study of timelike geodesic motion will be further divided into subsections, (i) timelike geodesic for radial motion of the particle, (ii) timelike geodesic for non-radial motion of the particle.

2.1 Geodesic Motion in Spherically Symmetric Static Spacetime

The general spherical symmetric static spacetime [38] is

$$ds^2 = -f(r)dt^2 + \frac{dr^2}{f(r)} + r^2(d\theta^2 + \sin^2\theta d\phi^2). \quad (2.1.1)$$

Consider the motion of a particle in equatorial plane, i.e. $\theta = \frac{\pi}{2}$, then the geodesic Lagrangian is

$$\mathcal{L} = \frac{1}{2} \left[-f(r)\dot{t}^2 + \frac{\dot{r}^2}{f(r)} + r^2(\dot{\phi}^2) \right]. \quad (2.1.2)$$

The Euler-Lagrange equations in general form are

$$\frac{d}{d\tau} \left(\frac{\partial \mathcal{L}}{\partial \dot{q}^\mu} \right) - \frac{\partial \mathcal{L}}{\partial q^\mu} = 0. \quad (\mu = 0, 1, 2, 3) \quad (2.1.3)$$

For $\mu = 0$ i.e. $q^0 = t$, the Euler-Lagrange equations (2.1.3) becomes

$$\frac{d}{d\tau} \left(\frac{\partial \mathcal{L}}{\partial \dot{t}} \right) - \frac{\partial \mathcal{L}}{\partial t} = 0. \quad (2.1.4)$$

There is no term involving 't' in the equation (2.1.2), so $\frac{\partial \mathcal{L}}{\partial t} = 0$. Thus equation (2.1.4) becomes

$$\frac{d}{d\tau} \left(\frac{\partial \mathcal{L}}{\partial \dot{t}} \right) = 0. \quad (2.1.5)$$

Integrating this we get

$$\frac{\partial \mathcal{L}}{\partial \dot{t}} = -\frac{\varepsilon}{m} = -E, \quad (2.1.6)$$

where 'E' denotes the energy of the test particle per unit mass, i.e. $E = \frac{\varepsilon}{m}$. Differentiating equation (2.1.2) with respect to \dot{t} , we get

$$\frac{\partial \mathcal{L}}{\partial \dot{t}} = -f(r)\dot{t}. \quad (2.1.7)$$

Comparing equation (2.1.6) with equation (2.1.7) we get

$$\dot{t} = \frac{E}{f(r)}. \quad (2.1.8)$$

Similarly ' $\dot{\phi}$ ' can be find from equation (2.1.2) and equation (2.1.3), as

$$\dot{\phi} = \frac{\ell}{r^2}. \quad (2.1.9)$$

Here ' ℓ ' represents the angular momentum per unit mass of the particle, i.e. $\ell = \frac{l}{m}$. Now we find ' \dot{r} ' by using the equation

$$-1 = -g_{tt}\dot{t}^2 + g_{rr}\dot{r}^2 + g_{\phi\phi}\dot{\phi}^2. \quad (2.1.10)$$

For the spherically symmetric static spacetime, equation (2.1.1) in equatorial plane becomes

$$-1 = -f(r)\dot{t}^2 + \frac{1}{f(r)}\dot{r}^2 + r^2\dot{\phi}^2. \quad (2.1.11)$$

By putting the values of \dot{t} and $\dot{\phi}$ from equations (2.1.8) and (2.1.9) in equation (2.1.11) we have

$$-1 = \frac{-E^2}{f(r)} + \frac{1}{f(r)}\dot{r}^2 + \frac{\ell^2}{r^2}. \quad (2.1.12)$$

Multiplying $f(r)$ on both sides of equation (2.1.12) and then rearranging the equation, we obtain

$$\dot{r}^2 = f(r) \left(-1 + \frac{E^2}{f(r)} - \frac{\ell^2}{r^2} \right), \quad (2.1.13)$$

or it can be written as

$$\dot{r} = \pm \sqrt{f(r) \left(-1 + \frac{E^2}{f(r)} - \frac{\ell^2}{r^2} \right)}. \quad (2.1.14)$$

All the 4-velocity components are represented by equations (2.1.8), (2.1.9) and (2.1.14) while $\dot{\theta} = 0$. In equation (2.1.14) the plus sign indicates the outgoing radial velocity of the particles while the negative sign indicate the ingoing radial velocity of the particles.

2.2 Timelike Geodesic Motion in Static Hořava-Lifshitz Black Holes

Consider again equation (2.1.1) and $f(r)$ as given in [39]

$$f(r) = 1 + (\omega - \Lambda_w)r^2 - \left(r[\omega(\omega - 2\Lambda_w)r^3 + \beta] \right)^{\frac{1}{2}}. \quad (2.2.1)$$

Here $f(r)$ is the lapse function $f(r) > 0$ which represents the time elapsed between two points and β is the integration constant, where $\omega = \frac{16\mu^2}{\kappa^2}$ is the coupling constant and Λ_w is the cosmological constant [40]. Here we have two special cases for the static or KS HL black hole.

Case-I

By putting $\beta = 4\omega M$ and $\Lambda_w = 0$, equation (2.2.1) reduces to case of KS black hole [38] i.e

$$f_{KS}(r) = 1 + \omega r^2 - (\omega^2 r^4 + 4\omega M r)^{\frac{1}{2}}, \quad (2.2.2)$$

from this we have

$$f_{KS}(r) = 1 + \omega r^2 - \sqrt{r(\omega^2 r^3 + 4\omega M)}. \quad (2.2.3)$$

Case-II

This case represents solution of Lu-Mei- Pope (LMP) black hole [37]. If $\beta = -\frac{\alpha^2}{\Lambda_w}$ and $\omega = 0$, then equation (2.2.1) gives the case of LMP black hole

$$f_{LMP} = 1 - \Lambda_w r^2 + \left(\frac{\alpha^2 r}{\Lambda_w}\right)^{\frac{1}{2}}. \quad (2.2.4)$$

Simplifying equation (2.2.4), this gives

$$f_{LMP} = 1 - \Lambda_w r^2 - \frac{\alpha}{\sqrt{-\Lambda_w}} \sqrt{r}. \quad (2.2.5)$$

Now we consider equation (2.2.2) which can be written as

$$f(r) = 1 + \omega r^2 - \omega r^2 \left(1 + \frac{4M}{\omega r^3}\right)^{\frac{1}{2}}. \quad (2.2.6)$$

Applying binomial expansion on the last term in equation (2.2.6), we get

$$\left(1 + \frac{4M}{\omega r^3}\right)^{\frac{1}{2}} = 1 + \frac{2M}{\omega r^3} + \frac{2M^2}{\omega^2 r^6} + \dots \quad (2.2.7)$$

Put this in equation (2.2.6) which becomes

$$f(r) = 1 + \omega r^2 - \omega r^2 \left(1 + \frac{2M}{\omega r^3} + \frac{2M^2}{\omega^2 r^6} + \dots\right). \quad (2.2.8)$$

By cancelation and neglecting the terms involving r^{-2} and r^{-4} equation (2.2.8) becomes

$$f(r) \approx 1 - \frac{2M}{r}. \quad (2.2.9)$$

In equation (2.2.9) ‘ M ’ is the integration constant, having dimensions of mass. Here $r \gg (\frac{M}{\omega})^{\frac{1}{3}}$ [39], which gives the usual behaviour of Schwarzschild black hole.

To find the event horizons equation (2.2.3) becomes

$$1 + \omega r^2 - \sqrt{r(\omega^2 r^3 + 4\omega M)} = 0, \quad (2.2.10)$$

Simplifying equation (2.2.10), which gives a quadratic equation in ‘ r ’

$$r^2 - 2Mr + \frac{1}{2\omega} = 0. \quad (2.2.11)$$

Solving this equation, we get two roots or event horizons which are

$$r_{\pm} = M \left(1 \pm \sqrt{1 - \frac{1}{2\omega M^2}} \right). \quad (2.2.12)$$

Applying binomial expansion and neglecting square and higher terms of ω involving in the expansion we arrive at

$$\left(1 - \frac{1}{2\omega M^2} \right)^{\frac{1}{2}} = 1 - \frac{1}{4\omega M^2}, \quad (2.2.13)$$

putting this in equation (2.2.12) we have

$$r_{\pm} = M \left(1 \pm \left[1 - \frac{1}{4\omega M^2} \right] \right), \quad (2.2.14)$$

where the outer horizon becomes

$$r_+ = M \left(1 + \left[1 - \frac{1}{4\omega M^2} \right] \right). \quad (2.2.15)$$

To avoid naked singularity $\omega M \geq \frac{1}{4}$. When $\omega M \gg 1$, means that according to the conventional GR rule, the horizon reaches to

$$r_+ \approx 2M - \frac{1}{2\omega M} + \dots \quad (2.2.16)$$

Thus the r_+ is lower than the usual Schwarzschild horizon, $r_{+Sch}=2M$, while the inner horizon tends to zero i.e $r_- \rightarrow 0$.

2.3 Timelike Geodesics for Static Black Hole in Hořava-Lifshitz Gravity

Here we review the timelike geodesics for a particle in the KS black hole spacetime. Here the equation (2.1.10) becomes

$$-h = -g_{tt}\dot{t}^2 + g_{rr}\dot{r}^2 + g_{\phi\phi}\dot{\phi}^2, \quad (2.3.1)$$

putting values of g_{tt} , g_{rr} , $g_{\phi\phi}$ from equation (2.1.11) where t and ϕ from equation (2.1.8) and equation (2.1.9) respectively, and simplifying

$$-h = \frac{-E^2}{1 + \omega r^2 - \sqrt{r(\omega^2 r^3 + 4\omega M)}} + \frac{\dot{r}^2}{1 + \omega r^2 - \sqrt{r(\omega^2 r^3 + 4\omega M)}} + \frac{\ell^2}{r^2}, \quad (2.3.2)$$

from this equation we have

$$-\left(h + \frac{\ell^2}{r^2}\right)\left(1 + \omega r^2 - \sqrt{r(\omega^2 r^3 + 4\omega M)}\right) = -E^2 + \dot{r}^2. \quad (2.3.3)$$

Equation (2.3.3) implies that

$$\dot{r}^2 = E^2 - \left(1 + \omega r^2 - \sqrt{r(\omega^2 r^3 + 4\omega M)}\right)\left(h + \frac{\ell^2}{r^2}\right), \quad (2.3.4)$$

or

$$\dot{r}^2 = E^2 - V_{eff}^2, \quad (2.3.5)$$

where

$$V_{eff}^2 = \left(1 + \omega r^2 - \sqrt{r(\omega^2 r^3 + 4\omega M)}\right)\left(h + \frac{\ell^2}{r^2}\right). \quad (2.3.6)$$

Here V_{eff}^2 is known as effective potential [39].

In the case of massive particle we put $h = 1$, then the effective potential for timelike geodesics becomes

$$V_{eff}^2 = \left(1 + \omega r^2 - \sqrt{r(\omega^2 r^3 + 4\omega M)}\right) \left(1 + \frac{\ell^2}{r^2}\right). \quad (2.3.7)$$

Here we discuss two cases i.e radial and non radial motion of the particle.

2.3.1 Timelike Geodesic for Radial Motion of Particles in Static Black Hole

In this case the particle's motion in the radial geodesic have no angular momentum, i.e $\ell = 0$. It means that particle comes from infinity to the center along the radial direction. In this case equation (2.3.7) becomes

$$V_{eff}^2 = 1 + \omega r^2 - \sqrt{r(\omega^2 r^3 + 4\omega M)}. \quad (2.3.8)$$

Figure (2.1) shows two lines, the bold line represents the effective potential of the particle motion for static black hole in the back ground geometry of HL gravity while the dashed line denotes schwarzschild effective potential. At large distances HL theory reduces to standard GR because the higher derivative does not contribute in the equation of motion. Therefore the effective potential for HL black hole matches to Schwarzschild black hole at large distances while for short distances it does not match as shown in the figure. From this graph it is also clear that the particle is pushed towards horizon from large distances which is determined by the energy ' E ' of the particle.

The equation for the radial motion (2.3.4) takes the form

$$\dot{r}^2 = E^2 - \left(1 + \omega r^2 - \sqrt{r(\omega^2 r^3 + 4\omega M)}\right). \quad (2.3.9)$$

In the graph (2.2) we see that at constant energy E , the velocity of the particle decreases and reaches to zero. When the particle comes to a finite distance, then the particle goes back

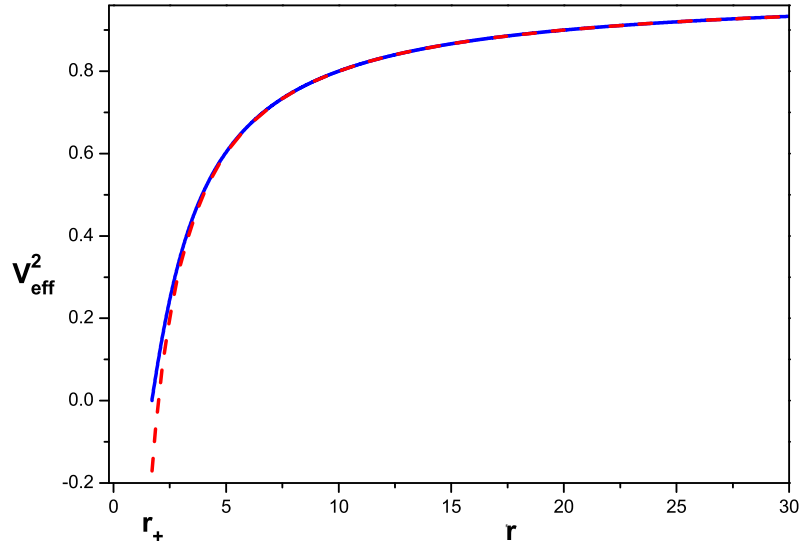


Figure 2.1: Plot for the equation (2.3.8) between V_{eff}^2 and r , with parameters $\ell = 0$, $\omega = 1$ and $M = 1$.

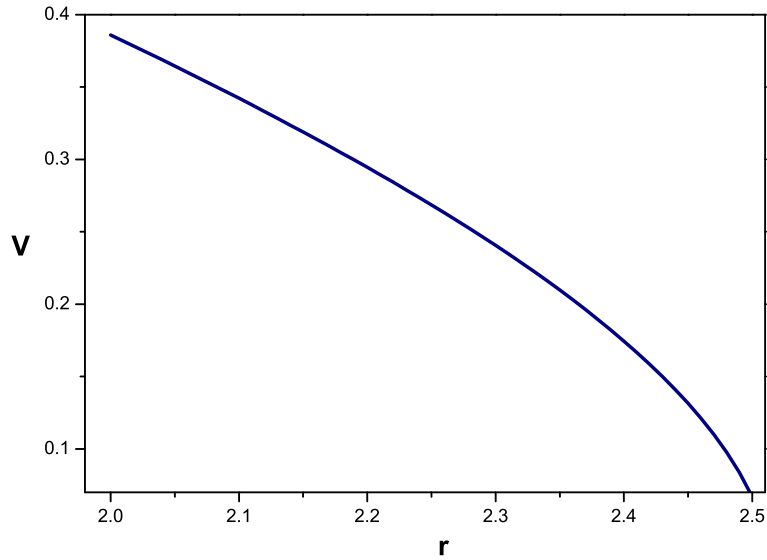


Figure 2.2: Plot of velocity v and distance r for equation (2.3.9) represents the radial motion of the particle with parameters $E = 0.5$, $\omega = 1$ and $M = 1$.

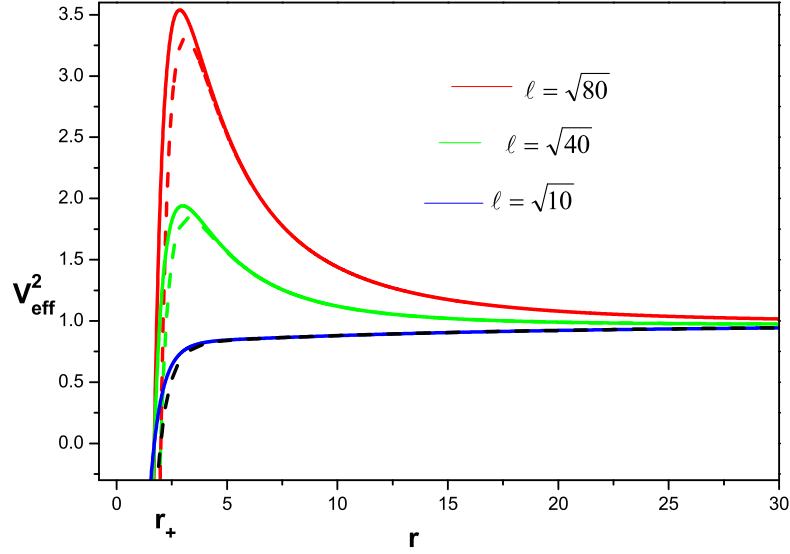


Figure 2.3: Plot for V_{eff}^2 vs r for equation (2.3.10) for non radial motion of the particle with various values of $\ell^2 = 80M^2$, $\ell^2 = 40M^2$ and $\ell^2 = 10M^2$ and with parameters $M = 1$, $\omega = 1$ and $h = 1$

and drop down into the center.

2.3.2 Timelike Geodesic for Non-radial Motion of Particles in Static Black Hole

In this case the angular momentum gets involved means that $\ell \neq 0$ and $h = 1$ then the equation (2.3.7) can be expressed as

$$V_{eff}^2 = \left(1 + \omega r^2 - \sqrt{r(\omega^2 r^3 + 4\omega M)}\right) \left(1 + \frac{\ell^2}{r^2}\right). \quad (2.3.10)$$

The Figure (2.3) shows that by increasing the value of ℓ the peak of the effective potential becomes sharper and sharper which means that the orbit of the particle becomes unstable.

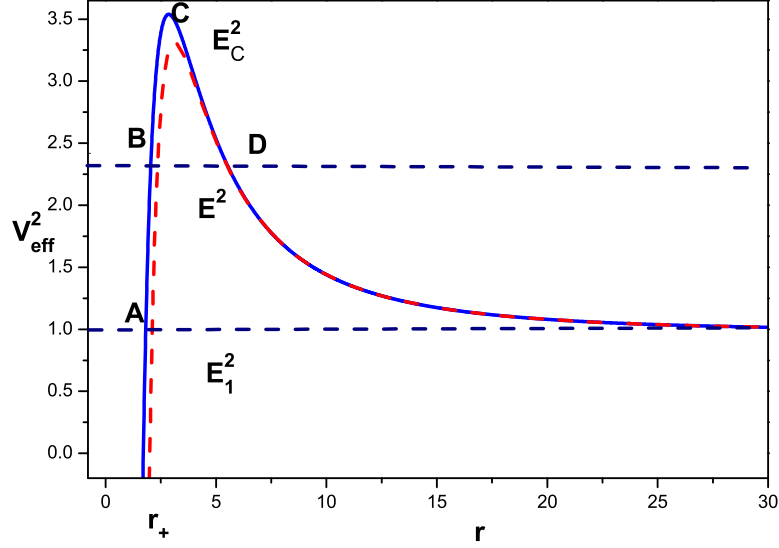


Figure 2.4: Plot between V_{eff}^2 and r for non radial motion of particles, for various values of $\ell^2 = 80M^2$ and with parameters $M = 1$, $\omega = 1$ and $h = 1$

For $\ell = \sqrt{10}$ the effective potential represents the unique stable orbit. While dashed lines represents the schwarzschild effective potential. The difference between effective potentials occurs at short distance because it does not match to standard GR while for large distance it becomes same because at large distances the HL theory reduces to standard GR as given in the figure.

In this case the non-radial equation of motion becomes

$$\dot{r}^2 = E^2 - \left(1 + \omega r^2 - \sqrt{r(\omega^2 r^3 + 4\omega M)}\right) \left(1 + \frac{\ell^2}{r^2}\right). \quad (2.3.11)$$

The Figure (2.4) represent plot for the equation (2.3.10) with $\ell^2 = 80M^2$. Effective potential for HL black hole matches at larger distances while it does not matches at shorter distances with Schwarzschild black hole as mention in the plot. Here are several cases due to different values of ‘ E ’ for non-radial case:

- (I) If $E^2 > E_C^2$, then the particle have enough energy, will jump directly from infinity into singularity. Here ‘ E ’ represents energy range denoted by dashed line while ‘ E_C ’ is the energy of the particle at point C , called critical energy as shown in the figure.
- (II) If $E^2 = E_C^2$, then orbit for non-radial motion of the particle is unstable at $r = r_C$. For this case the particle will escape to infinity at $r = r_C$, or fall into the singularity. Here r_C represents radial distance of the particle at point C .
- (III) If $E_1^2 < E^2 < E_C^2$, then the non-radial motion of the particle in such orbits will redirected from $r = r_D$, to infinity, or jump into the singularity from $r = r_B$. Here r_B and r_D represents the distance of radial motion of the particle at location B and D respectively given in the figure.
- (IV) If $E^2 > E_1^2$, then the non-radial motion of the particle will go directly into singularity, here E_1 denotes the proper energy range as shown by the lower dashed line in the figure. Below this range the particle’s motion becomes in the bounded region.

Chapter 3

Motion of a Particle in the Vicinity of Slowly Rotating Hořava-Lifshitz Black Hole

In this chapter timelike and null geodesic motion for a slowly rotating HL black hole is discussed. This is further subdivided into two sections (i) radial motion and (ii) non radial motion.

3.1 Geodesic Motion in Slowly Rotating Spacetime

Here we have an axisymmetric metric [39] as

$$ds^2 = -f(r)dt^2 + \frac{dr^2}{f(r)} + r^2 d\theta^2 + r^2 \sin^2 \theta (d\phi - aNdt)^2, \quad (3.1.1)$$

In the given metric (3.1.1) $a = \frac{J}{M}$, is the spin parameter. Here J is the spin angular momentum and M is the mass of the black hole, while $N = \frac{2M}{r^3}$ is the shift function. Where $f(r)$ shows the lapse function represented by equation (2.2.3) in chapter 2. In order to get slowly rotating black hole solution we have to keep equations of motion up to linear order in

a to obtain solution for the slowly rotating black hole. For this simplifying equation (3.1.1), where the motion is in equatorial plane (discussed in chapter 2), we have

$$ds^2 = -f(r)dt^2 + \frac{dr^2}{f(r)} + r^2(d\phi^2 - 2aNdt d\phi). \quad (3.1.2)$$

Its geodesic Lagrangian becomes

$$\mathcal{L} = \frac{1}{2} \left[-f(r)\dot{t}^2 + \frac{\dot{r}^2}{f(r)} + r^2(\dot{\phi}^2 - 2aN\dot{\phi}\dot{t}) \right]. \quad (3.1.3)$$

To find ' \dot{t} ' we use equation (2.1.5) in chapter 2, which gives

$$\frac{\partial \mathcal{L}}{\partial \dot{t}} = -\frac{\varepsilon}{M} = -E. \quad (3.1.4)$$

Differentiating equation (3.1.3) with respect to ' \dot{t} ' we obtain

$$\frac{\partial \mathcal{L}}{\partial \dot{t}} = [-f(r)\dot{t} - aNr^2\dot{\phi}], \quad (3.1.5)$$

replace $\frac{\partial \mathcal{L}}{\partial \dot{t}}$ by $-E$ in equation (3.1.5) we get

$$-E = [-f(r)\dot{t} - aNr^2\dot{\phi}], \quad (3.1.6)$$

simplifying equation (3.1.6) we arrive at the result

$$\dot{t} = \frac{E - aNr^2\dot{\phi}}{f(r)}. \quad (3.1.7)$$

Following the same procedure for ' $\dot{\phi}$ ' we find

$$\frac{\partial \mathcal{L}}{\partial \dot{\phi}} = \frac{l}{m} = \ell. \quad (3.1.8)$$

Differentiating equation (3.1.3) with respect to ' $\dot{\phi}$ ' we obtain

$$\frac{\partial \mathcal{L}}{\partial \dot{\phi}} = r^2\dot{\phi} - aNr^2\dot{t}, \quad (3.1.9)$$

putting $\frac{\partial L}{\partial \dot{\phi}} = \ell$ and also value of ' \dot{t} ' from equation (3.1.7) into equation (3.1.9) we get

$$\ell = r^2 \dot{\phi} - aNr^2 \left[\frac{E - aNr^2 \dot{\phi}}{f(r)} \right]. \quad (3.1.10)$$

Simplifying this equation we get

$$\dot{\phi} = \frac{aNr^2 E + \ell f(r)}{r^2 f(r)}. \quad (3.1.11)$$

Replace equation (3.1.11) in equation (3.1.7), then by linearizing (neglecting higher orders in a) we get

$$\dot{t} = \frac{E - aN\ell}{f(r)}. \quad (3.1.12)$$

To obtain \dot{r} , here equation (2.1.10) becomes

$$-f(r)\dot{t}^2 + f(r)^{-1}\dot{r}^2 + r^2\dot{\phi}^2 - 2ar^2N\dot{\phi}\dot{t} = -1. \quad (3.1.13)$$

Inserting values from equation (3.1.11) and equation (3.1.12) into equation (3.1.13) and rearrange we obtain

$$f(r)^{-1}\dot{r}^2 = \left[-1 + \left(f(r) \right) \left(\frac{E - aN\ell}{f(r)} \right)^2 - r^2 \left(\frac{aNr^2 E + \ell f(r)}{r^2 f(r)} \right)^2 \right], \quad (3.1.14)$$

simplifying this we get

$$\dot{r} = \pm \sqrt{f(r) \left(-1 + \frac{E^2}{f(r)} - \frac{\ell^2}{r^2} - \frac{2aN\ell E}{f(r)} \right)}. \quad (3.1.15)$$

So the 4-velocity components are represented by equations (3.1.11), (3.1.12) and (3.1.15), while $\dot{\theta} = 0$. Here the (+) sign shows the outgoing radial velocity of the particles, where as the (-) sign represents the incoming radial velocity of the particles.

3.2 Timelike Geodesics for Slowly Rotating Black Hole in Hořava-Lifshitz Gravity

Equation (3.1.13) for timelike geodesics takes the form

$$-h = [-f(r)\dot{t}^2 + f(r)^{-1}\dot{r}^2 + r^2\dot{\phi}^2 + 2aNr^2\dot{t}\dot{\phi}], \quad (3.2.1)$$

using values of \dot{t} and $\dot{\phi}$ from equation (3.1.11) and equation (3.1.12) in equation (3.2.1) we have

$$-h = -f(r)\left(\frac{E - aN\ell}{f(r)}\right)^2 + f(r)^{-1}\dot{r}^2 + r^2\left(\frac{aNEr^2 + \ell f(r)}{f(r)}\right)^2 + 2aN\left(\frac{E - aN\ell}{f(r)}\right)\left(\frac{aNr^2E + \ell f(r)}{f(r)}\right), \quad (3.2.2)$$

simplifying and rearranging equation (3.2.2) and reducing linear terms in 'a' we get

$$f(r)^{-1}\dot{r}^2 = \frac{E^2}{f(r)} - \frac{2aN\ell E}{f(r)} - \left(h + \frac{\ell^2}{r^2}\right), \quad (3.2.3)$$

for the case of massive particle we put $h = 1$ and multiplying $f(r)$ on both sides of equation (3.2.3)

$$\dot{r}^2 = f(r)\left[-1 + \frac{E^2}{f(r)} - \frac{\ell^2}{r^2} - \frac{2aN\ell E}{f(r)}\right], \quad (3.2.4)$$

which is similar to equation (3.1.15). Consider equation (3.2.3) in the form

$$\dot{r}^2 = E^2 - \left(1 + \omega r^2 - \sqrt{r(\omega^2 r^3 + 4\omega M)}\right)\left(h + \frac{\ell^2}{r^2}\right) - 2aN\ell E. \quad (3.2.5)$$

Where lapse function $f(r) = (1 + \omega r^2 - \sqrt{r(\omega^2 r^3 + 4\omega M)})$. In this case the effective potential will be

$$V_{eff}^2 = \left(1 + \omega r^2 - \sqrt{r(\omega^2 r^3 + 4\omega M)}\right)\left(h + \frac{\ell^2}{r^2}\right) - 2aN\ell E. \quad (3.2.6)$$

Inserting value of $h = 1$ in effective potential equation (3.2.6) we get

$$V_{eff}^2 = \left(1 + \omega r^2 - \sqrt{r(\omega^2 r^3 + 4\omega M)}\right)\left(1 + \frac{\ell^2}{r^2}\right) - 2aN\ell E, \quad (3.2.7)$$

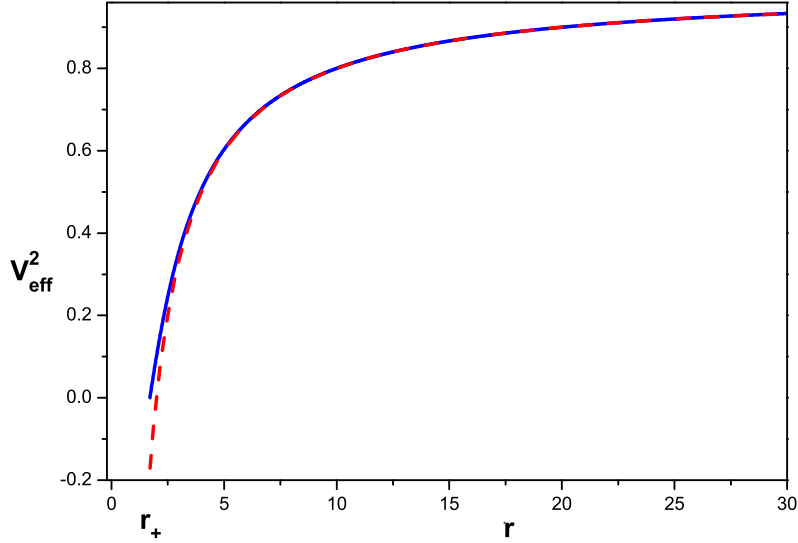


Figure 3.1: Graph for equation (3.2.8) of V_{eff}^2 vs r with parameters $\omega = 1$ and $M = 1$

3.2.1 Timelike Geodesic for Radial Motion of the Particle in Slowly rotating Black Hole

putting $\ell = 0$ in equation (3.2.7) we obtain

$$V_{\text{eff}}^2 = (1 + \omega r^2 - \sqrt{r(\omega^2 r^3 + 4\omega M)}), \quad (3.2.8)$$

The Figures (3.1) and (3.2) show two lines, the bold line represents the effective potential of the particle for rotating black hole in the back ground geometry of HL gravity while the dashed line denotes schwarzschild effective potential. At large distances HL theory reduces to standard GR because the higher derivative does not contribute in the equation of motion. The effective potential for HL black hole matches to Schwarzschild black hole at large distances while for short distances it does not match as shown in the figure. This figure also shows that the particle goes towards horizon from an upper range energy E , determined by the energy of the particle.

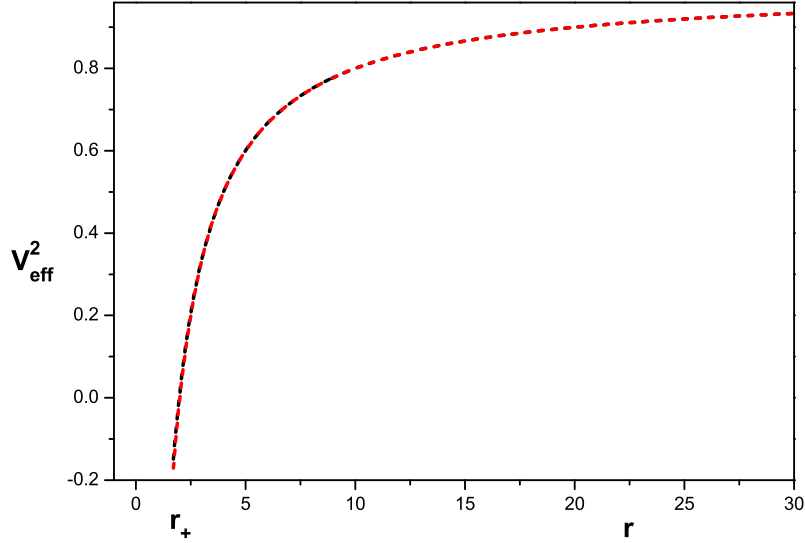


Figure 3.2: Graph for equation (3.2.8) of V_{eff}^2 vs r with parameters $\omega = 10$ and $M = 1$

Equation of radial motion becomes

$$\dot{r}^2 = E^2 - \left(1 + \omega r^2 - \sqrt{r(\omega^2 r^3 + 4\omega M)}\right). \quad (3.2.9)$$

In the graphs (3.3) and (3.4) we see that at constant energy E , the velocity of the particle approaches to zero. When the particle reaches to a finite distance, then the particle goes back and fall into the center.

3.2.2 Timelike Geodesic for Non-radial Motion of Particles in Slowly Rotating Black Hole

Here $\ell \neq 0$ and replace $N = \frac{2M}{r^3}$ in equation (3.2.7), i.e. for non radial motion of the particle case

$$V_{eff}^2 = \left(1 + \omega r^2 - \sqrt{r(\omega^2 r^3 + 4\omega M)}\right) \left(1 + \frac{\ell^2}{r^2}\right) - \frac{4aM\ell E}{r^3}. \quad (3.2.10)$$

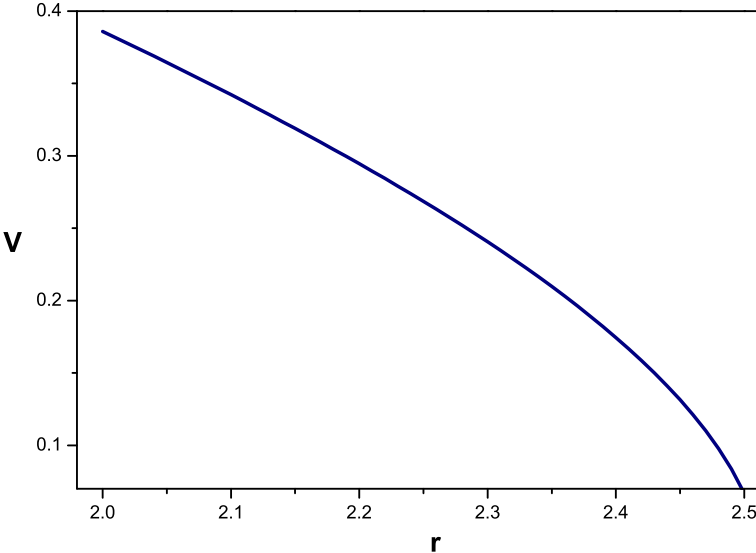


Figure 3.3: Graph of v vs r for equation (3.2.9) with $\omega = 1, M = 1$ and $E = 0.5$.

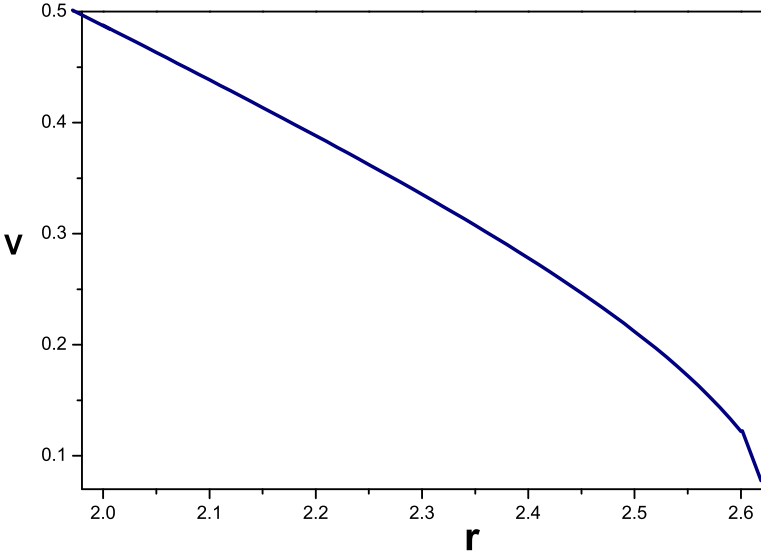


Figure 3.4: Graph of v vs r for equation (3.2.9) with $\omega = 10, M = 1$ and $E = 0.5$.

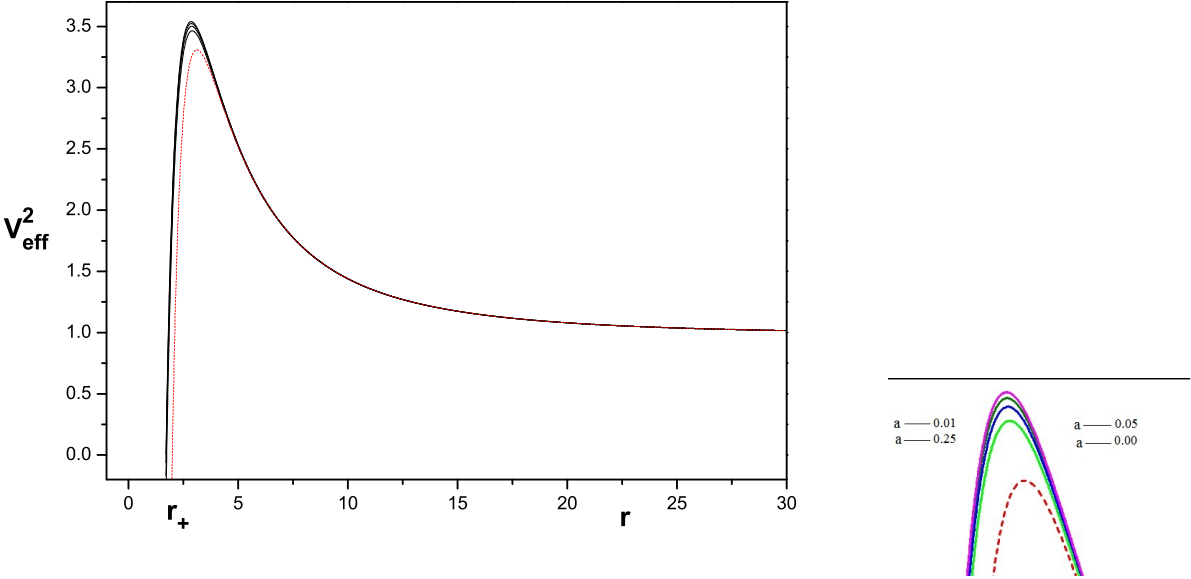


Figure 3.5: Graph for equation (3.2.10) of V_{eff}^2 vs r with parameters $\omega = 1, M = 1, E = 1$ and $\ell^2 = 80M^2$

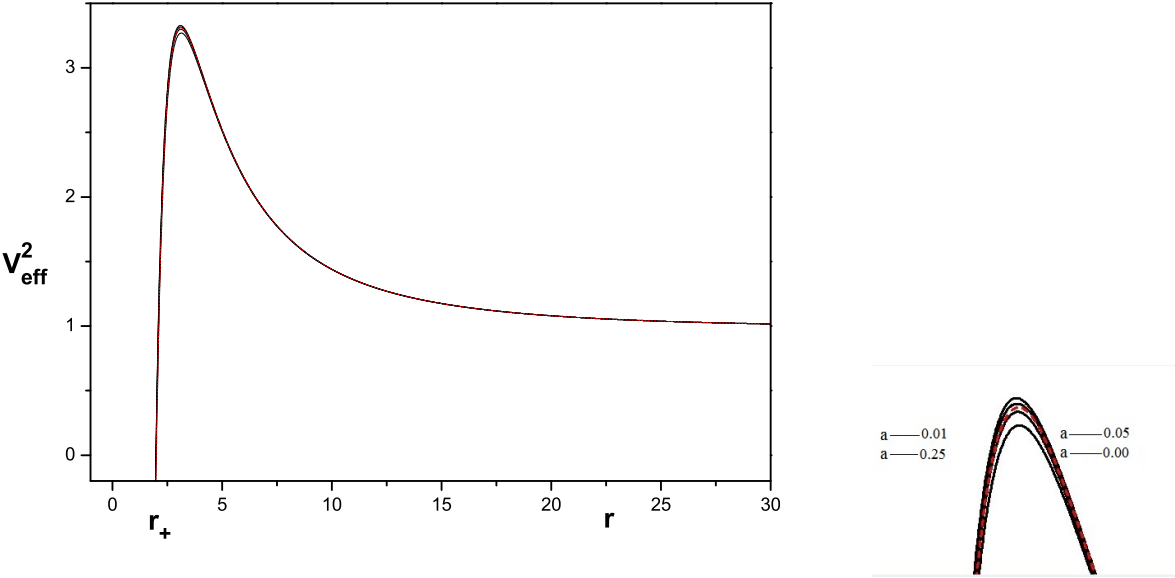


Figure 3.6: Graph for equation (3.2.10) of V_{eff}^2 vs r with parameters $\omega = 10, M = 1, E = 1$ and $\ell^2 = 80M^2$

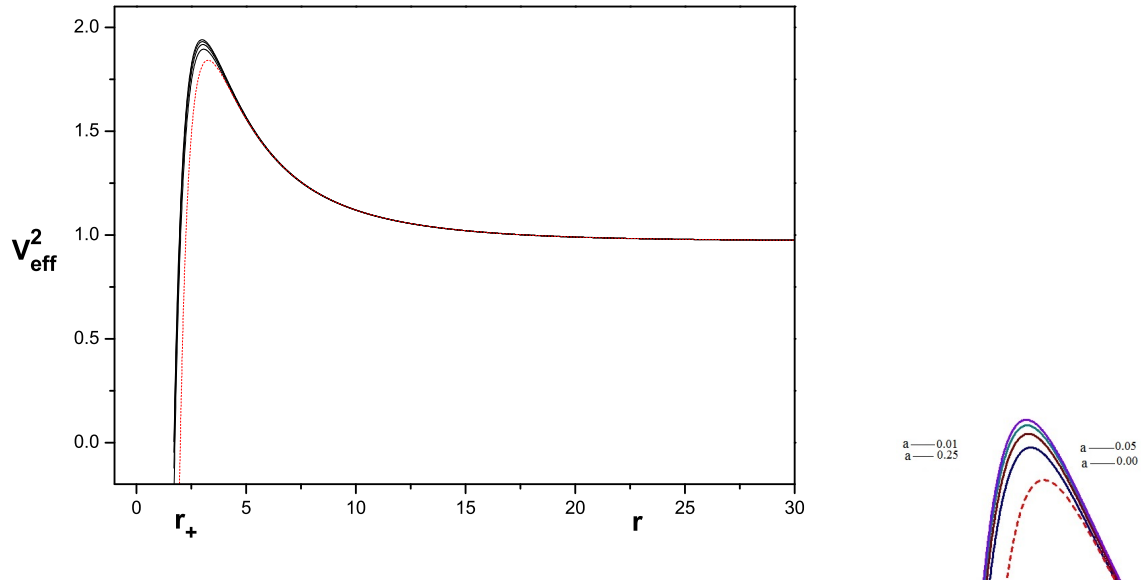


Figure 3.7: Graph for equation (3.2.10) of V_{eff}^2 vs r with parameters $\omega = 1, M = 1, E = 1$ and $\ell^2 = 40M^2$

The Figures (3.5) and (3.6) shows us the effective potential for HL black hole when $\ell^2 = 80M^2$. When the peak gets higher and higher, so the particle goes to unstable orbit. This means that instability of the orbit increases. Here the dashed line shows the Schwarzschild's effective potential while bold line shows the HL black hole effective potential. Initially there arises a difference in effective potential for HL black hole theory and Schwarzschild black hole at short distances while at end (large distances) it becomes same as shown in the graph. At the end both theories become equal so therefore the difference vanishes.

The Figures (3.7) and (3.8) shows us the effective potential for HL black holes for $\ell^2 = 40M^2$. As the peak becomes sharper, it means that the particle goes towards instable regions. Here the bold line represents the HL black hole effective potential while the dashed line represents the Schwarzschild's effective potential. The HL theory becomes equal to local GR in large distances while they do not match at short distances therefore at first there is a space in the effective potentials of HL theory and Schwarzschild as shown in the graph.

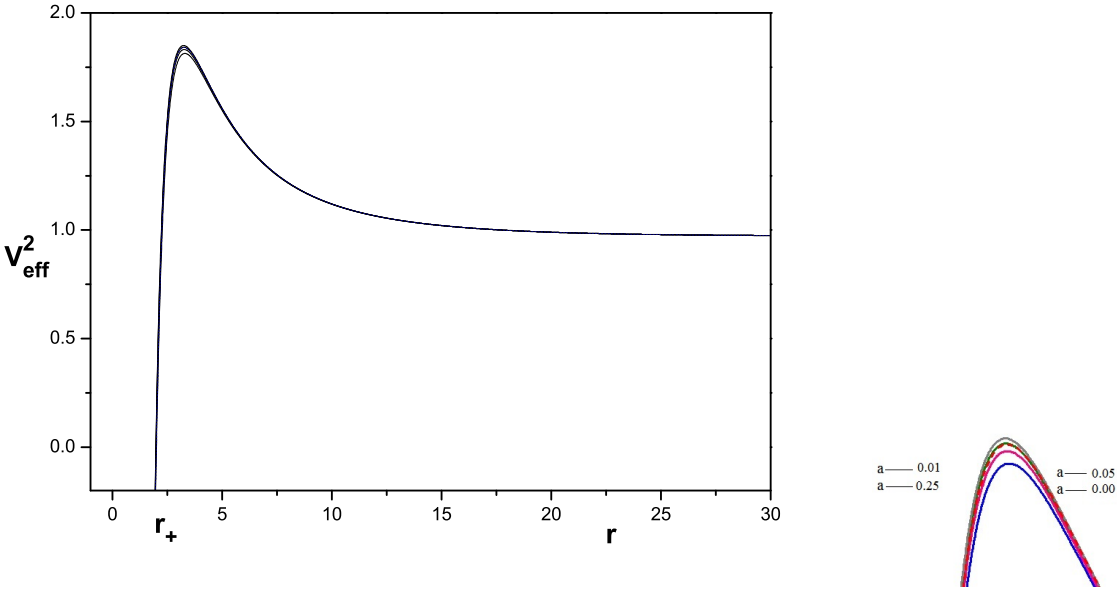


Figure 3.8: Graph for equation (3.2.10) of V_{eff}^2 vs r with parameters $\omega = 10, M = 1, E = 1$ and $\ell^2 = 40M^2$

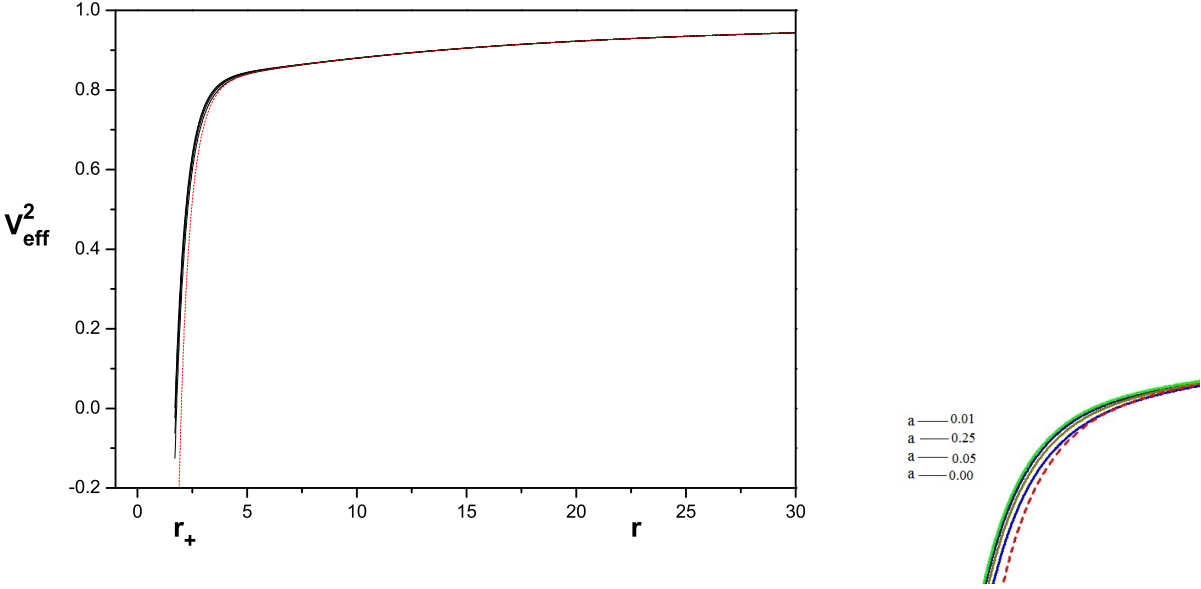


Figure 3.9: Graph for equation (3.2.10) of V_{eff}^2 vs r with parameters $\omega = 1, M = 1, E = 1$ and $\ell^2 = 10M^2$

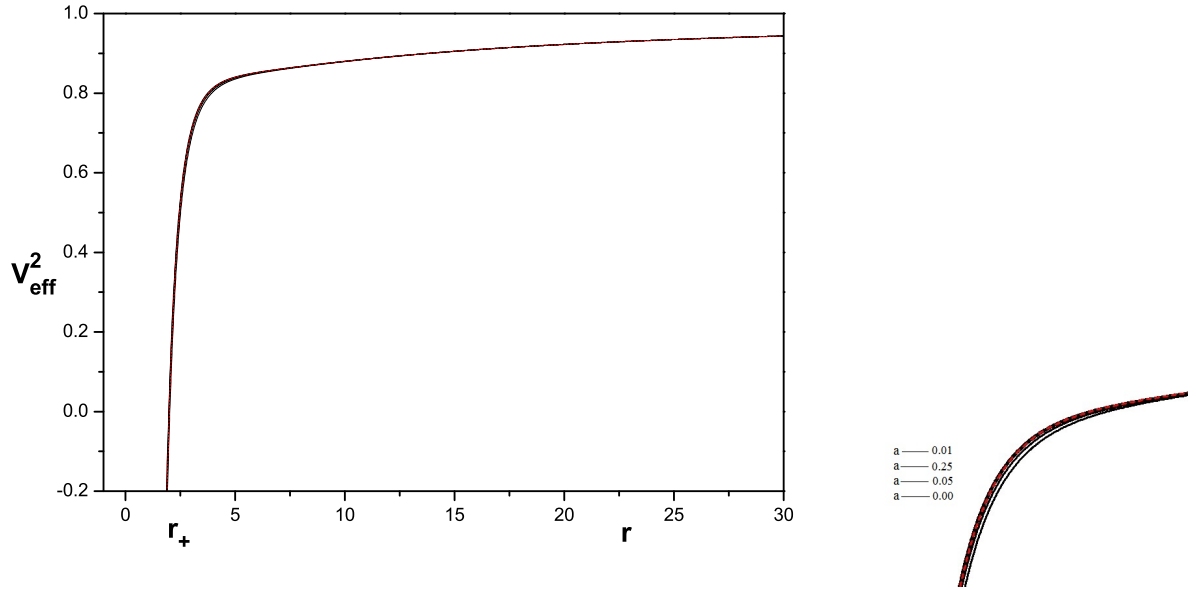


Figure 3.10: Graph for equation (3.2.10) of V_{eff}^2 vs r with parameters $\omega = 10$, $M = 1$, $E = 1$ and $\ell^2 = 10M^2$

The Figures (3.9) and (3.10) reflects about the effective potential for HL black hole if $\ell^2 = 10M^2$. In the given graph when the peaks become sharpens which reveals that the particle goes to unstable orbits. Here Schwarzschild's effective potential is represented by dashed line while bold line represents effective potential for the HL black hole. As stated above that the HL theory incorporates with standard GR at large distances while at shorter distances it does not, therefore the difference occurs at start as manifest in the figure.

Then for non-radial motion equation for the particle becomes

$$\dot{r}^2 = E^2 - \left(1 + \omega r^2 - \sqrt{r(\omega^2 r^3 + 4\omega M)}\right) \left(1 + \frac{\ell^2}{r^2}\right) - \frac{4aM\ell E}{r^3}. \quad (3.2.11)$$

3.3 Null Geodesics for Slowly Rotating Black Hole in Hořava-Lifshitz Gravity

Insert $h = 0$ in equation (3.2.6) then the effective potential becomes

$$V_{eff}^2 = \left(1 + \omega r^2 - \sqrt{r(\omega^2 r^3 + 4\omega M)}\right) \left(\frac{\ell^2}{r^2}\right) - \frac{4aM\ell E}{r^3}. \quad (3.3.1)$$

3.3.1 Null Geodesic for Radial Motion of Particles in Slowly Rotating Black Hole

For radial motion of the particle put $\ell = 0$ in equation (3.3.1) we obtain

$$V_{eff}^2 = 0. \quad (3.3.2)$$

Where the equation for radial motion of the particle become as

$$\dot{r}^2 = E^2. \quad (3.3.3)$$

The Figures (3.11) and (3.12) reveal the effective potential for HL black holes where $\ell^2 = 80M^2$. Here the dashed line tells us about the Schwarzschild's effective potential while bold line is for the effective potential of HL black hole. The HL theory reduces to standard GR while at shorter distances it does not reduce, therefore there originate a difference between Schwarzschild effective potential and HL black hole effective potential as shown in the figure.

For non radial case there arises different cases due to energy of the particle which is as follow:

(I) If $E^2 > E_c^2$, then the particle have enough energy and will go directly from infinity and jump into singularity.

(II) If $E^2 = E_c^2$, then orbit of the non-radial motion of the particle becomes unstable at $r = r_c$. In this case the particle will escape to infinity at $r = r_c$, or to singularity.

(III) If $E_1^2 < E^2 < E_c^2$, here the non-radial motion of the particle in such orbits will redirected from $r = r_D$ to infinity, or to singularity from $r = r_B$.

(IV) If $E^2 > E_1^2$, then the particle will jump directly into singularity.

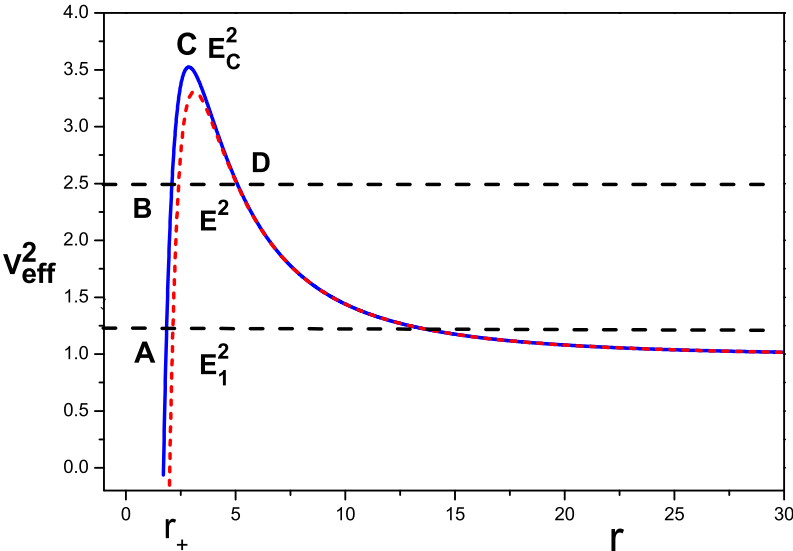


Figure 3.11: Graph of V_{eff}^2 vs r for equation (3.3.1) with parameters $\omega = 1, M = 1, E = 1$ and $\ell^2 = 80M^2$

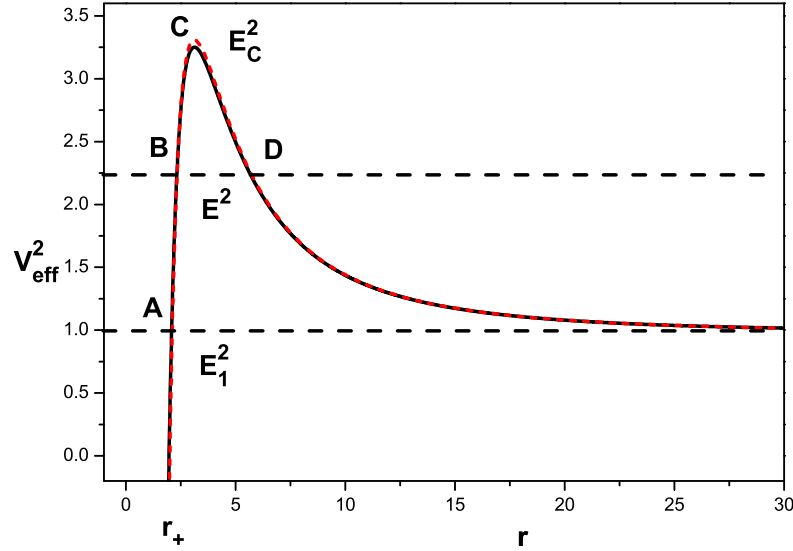


Figure 3.12: Graph of V_{eff}^2 vs r for equation (3.3.1) with parameters $\omega = 10, M = 1, E = 1$ and $\ell^2 = 80M^2$

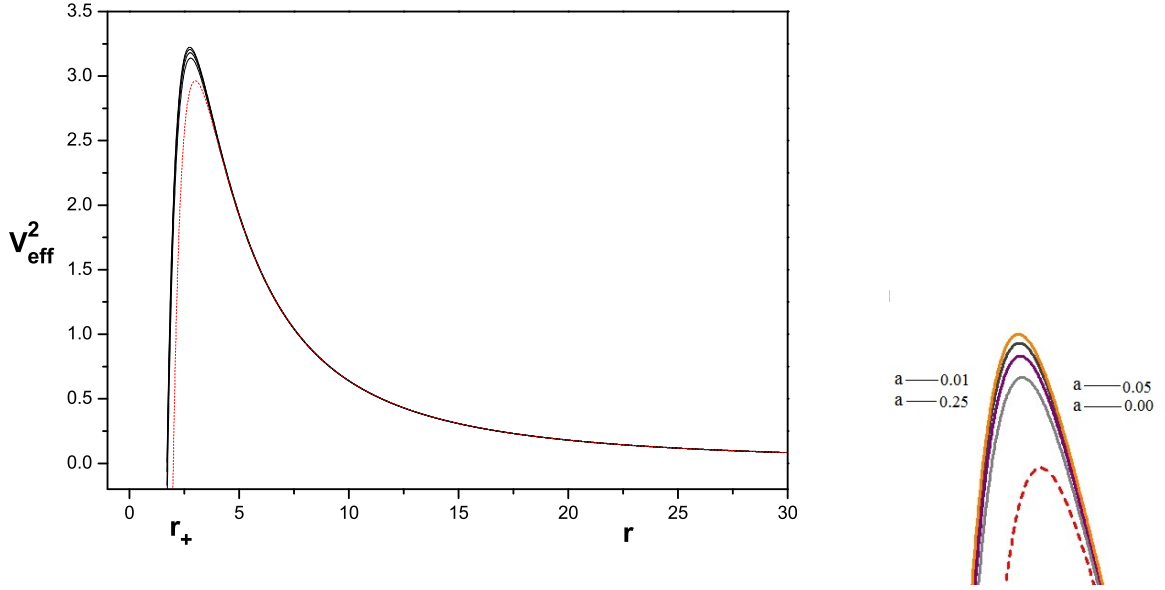


Figure 3.13: Graph for equation (3.3.4) of V_{eff}^2 vs r with parameters $\omega = 1, M = 1, E = 1$ and $\ell^2 = 80M^2$

3.3.2 Null Geodesic for Non-radial Motion of Particles in Slowly Rotating Black Hole

Put $\ell \neq 0$ for the non radial motion of the the particle case then equation (3.3.1) becomes

$$V_{eff}^2 = \left(1 + \omega r^2 - \sqrt{r(\omega^2 r^3 + 4\omega M)} \right) \left(\frac{\ell^2}{r^2} \right) - \frac{4aM\ell E}{r^3}. \quad (3.3.4)$$

The Figures (3.13) and (3.14) tells us that as the peaks become sharper and sharper, means that the instability of the orbit increases. Here the Schwarzschild's effective potential is denoted by dashed line while the bold line represents the HL black hole effective potential. In the beginning there is a discrimination between Schwarzschild's effective potential and HL black hole effective potential. This discrimination gradually decreases and finally emerges into a single line, which shows that HL theory matches to standard GR at large distances as shown in the graph. This graph is for $\ell^2 = 80M^2$.

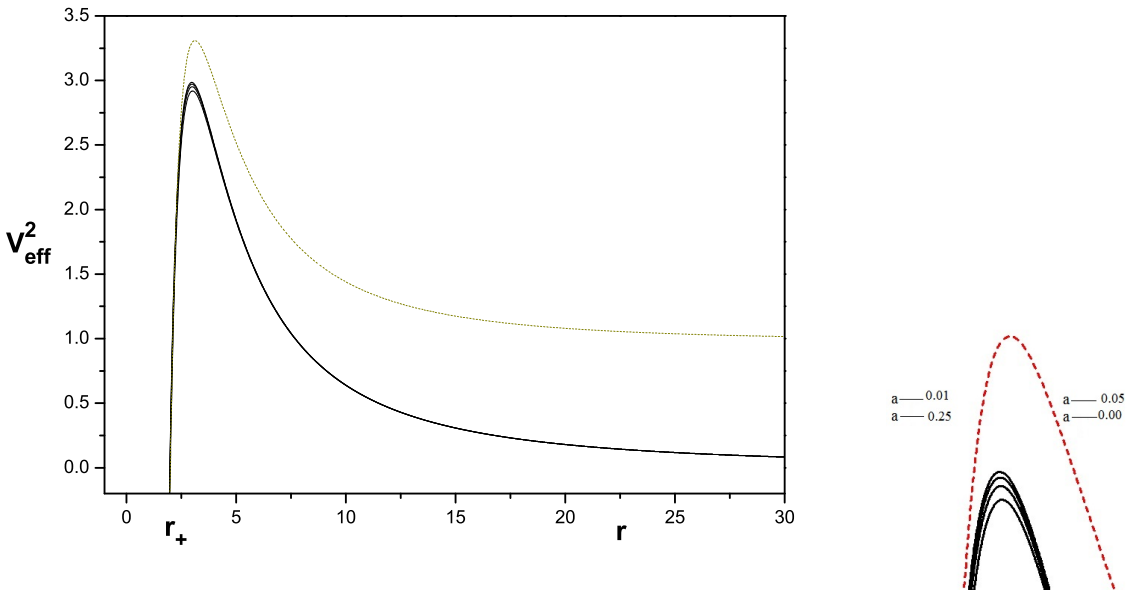


Figure 3.14: Graph for equation (3.3.4) of V_{eff}^2 vs r with parameters $\omega = 10, M = 1, E = 1$ and $\ell^2 = 80M^2$

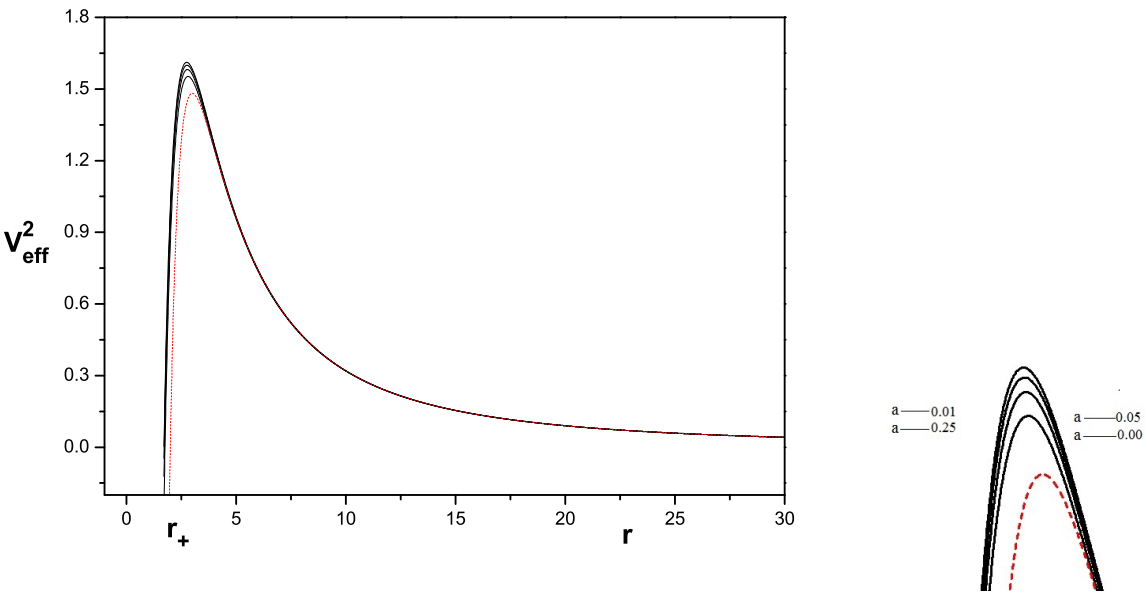


Figure 3.15: Graph for equation (3.3.4) of V_{eff}^2 vs r with parameters $\omega = 1, M = 1, E = 1$ and $\ell^2 = 40M^2$

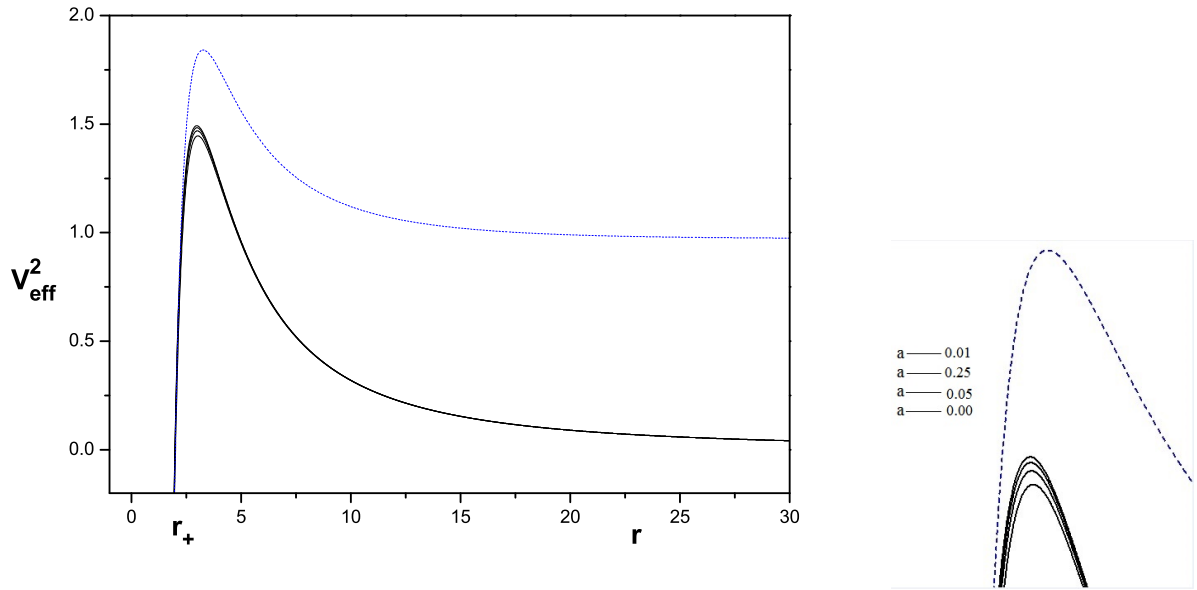


Figure 3.16: Graph for equation (3.3.4) of V_{eff}^2 vs r with parameters $\omega = 10, M = 1, E = 1$ and $\ell^2 = 40M^2$

The Figures (3.15) and (3.16) shows the effective potential for $\ell^2 = 40M^2$ and different values of a . In these graphs the peaks get sharper which shows that the instability of the orbit increases. Here the dashed line is for the Schwarzschild’s effective potential while bold line stands for the HL black hole effective potential. This graph shows that HL theory deviate from standard GR in the start and then becomes same in the end. This is shown for $\ell^2 = 40M^2$.

In the Figures (3.17) and (3.18) it is shown in graphs that the peaks become sharpens this reflects that the orbit instability increases. It means that the particle goes to unstable orbits. Here the dashed line shows the Schwarzschild’s effective potential while bold line represents the HL black hole effective potential. At short distances the HL theory diverges from standard GR while at large distances both theories converges into a single which is shown in the figure. This plot is for $\ell^2 = 10M^2$.

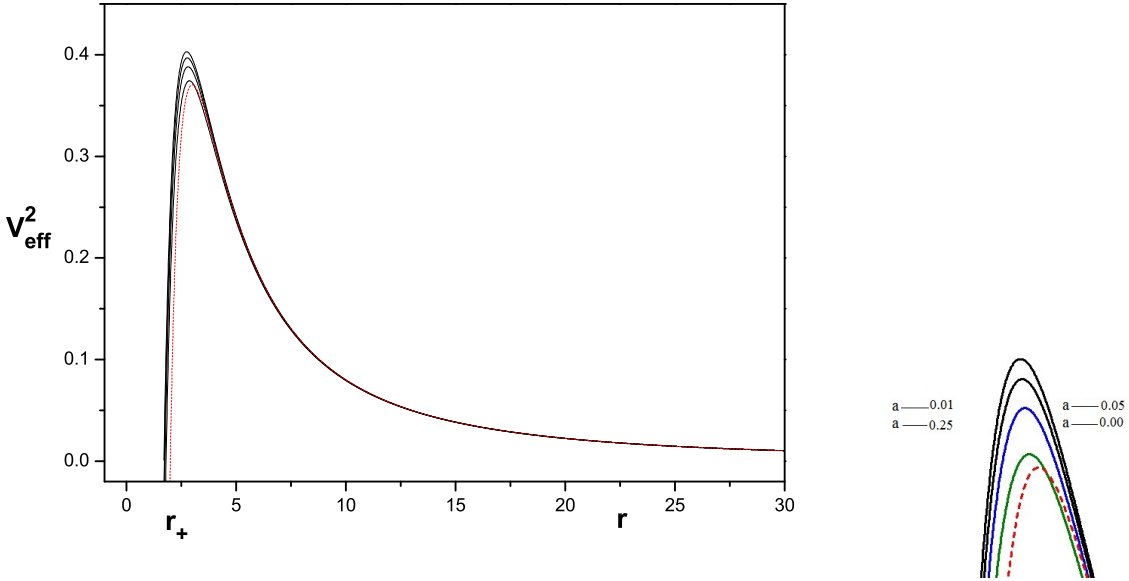


Figure 3.17: Graph for equation (3.3.4) of V_{eff}^2 vs r with parameters $\omega = 1, M = 1, E = 1$ and $\ell^2 = 10M^2$

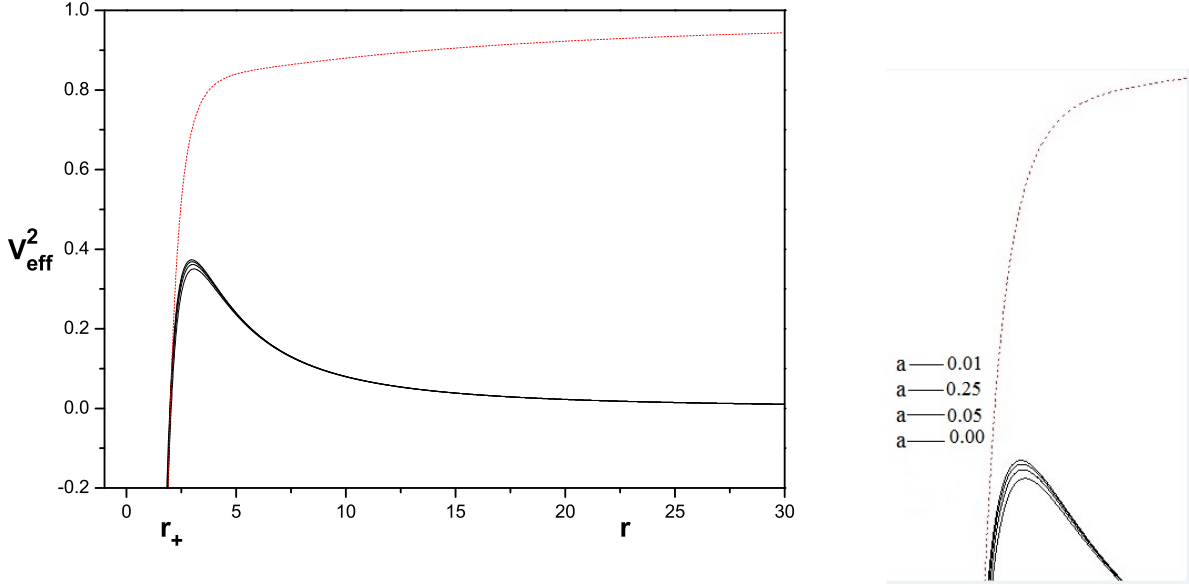


Figure 3.18: Graph for equation (3.3.4) of V_{eff}^2 vs r with parameters $\omega = 10, M = 1, E = 1$ and $\ell^2 = 10M^2$

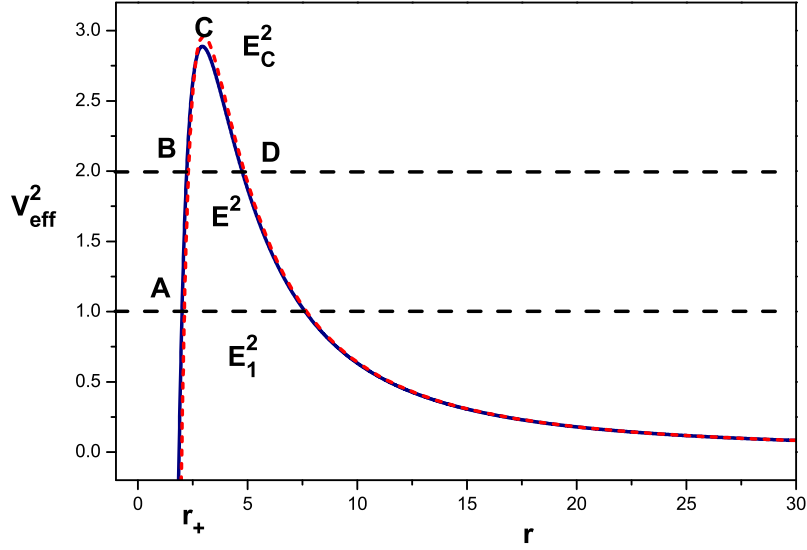


Figure 3.19: Graph of V_{eff}^2 vs r with parameters $\omega = 1$, $M = 1$, $E = 1$ and $\ell^2 = 80M^2$

For this case the equation for non-radial motion of the particle becomes

$$\dot{r}^2 = E^2 - \left(1 + \omega r^2 - \sqrt{r(\omega^2 r^3 + 4\omega M)} \right) \left(\frac{\ell^2}{r^2} \right) - \frac{4aM\ell E}{r^3}. \quad (3.3.5)$$

The Figures (3.19) and (3.20) show us the effective potential for HL black holes when $\ell^2 = 80M^2$. Here the dotted line is for the Schwarzschild's effective potential while bold line shows the HL black hole effective potential. The HL theory becomes equal to standard GR at large distances while they does not match with each other at shorter distances so therefore there arises a difference which is shown in the graph. Due to energy of the particle for non-radial case there arises different cases:

(I) If $E^2 > E_c^2$, then the particle have enough energy and will jump from infinity and fall into singularity.

(II) If $E^2 = E_c^2$, then orbit becomes unstable for non-radial motion of the particle at $r = r_c$. Here in these situations the particle will escape to infinity at $r = r_c$, or captured in the singularity.

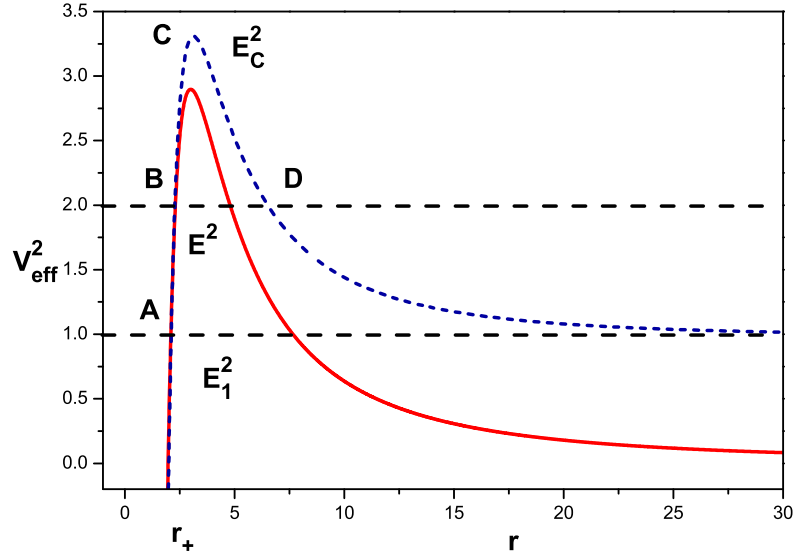


Figure 3.20: Graph of V_{eff}^2 vs r with parameters $\omega = 10$, $M = 1$, $E = 1$ and $\ell^2 = 80M^2$

- (III) If $E_1^2 < E^2 < E_c^2$, In such orbits the particle's non-radial motion will be redirected from $r = r_D$ to infinity, or to singularity from $r = r_B$.
- (IV) If $E^2 > E_1^2$, thus the particle will go directly and fall into singularity.

3.4 Velocity of the Particle

For velocity we have to divide \dot{r} by \dot{t} where

$$\dot{r} = \sqrt{f(r) \left(-h + \frac{E^2}{f(r)} - \frac{\ell^2}{r^2} - \frac{2aN\ell E}{f(r)} \right)}, \quad (3.4.1)$$

and second equation becomes as

$$\dot{t} = \frac{E - aN\ell}{f(r)}, \quad (3.4.2)$$

where

$$v = \frac{\dot{r}}{\dot{t}}, \quad (3.4.3)$$

now putting values of \dot{r} and \dot{t} from equation (3.4.1) and equation (3.4.2) into equation (3.4.3) we have

$$v = \frac{\sqrt{f(r) \left(-h + \frac{E^2}{f(r)} - \frac{\ell^2}{r^2} - \frac{2aN\ell E}{f(r)} \right)}}{\frac{E-aN\ell}{f(r)}}, \quad (3.4.4)$$

simplifying this equation we obtain

$$v = f^2(r) \sqrt{E^2 - f(r) \left(\frac{\ell^2}{r^2} \right)} \left[1 - \left(\frac{h}{f(r) \left(E^2 - f(r) \left(\frac{\ell^2}{r^2} \right) \right)} + \frac{2aN\ell E}{f^2(r) \left(E^2 - f(r) \left(\frac{\ell^2}{r^2} \right) \right)} \right) \right]^{\frac{1}{2}} [E^{-1}] \left[1 - \frac{aN\ell}{E} \right]^{-1}. \quad (3.4.5)$$

Expanding second and last term through binomial expansion and then simplifying we get

$$v = \left[1 - \frac{h}{2f(r) \left(E^2 - f(r) \left(\frac{\ell^2}{r^2} \right) \right)} - \frac{aN\ell E}{f^2(r) \left(E^2 - f(r) \left(\frac{\ell^2}{r^2} \right) \right)} + \frac{aN\ell}{E} - \frac{aN\ell h}{2Ef^2(r) \left(E^2 - f(r) \left(\frac{\ell^2}{r^2} \right) \right)} \right] \times [E^{-1}] f(r) \sqrt{E^2 - f(r) \left(\frac{\ell^2}{r^2} \right)} \quad (3.4.6)$$

3.5 Timelike Geodesics

By putting $h = 1$ in equation (3.4.6) we have

$$v = \left[1 - \frac{1}{2f(r) \left(E^2 - f(r) \left(\frac{\ell^2}{r^2} \right) \right)} - \frac{aN\ell E}{f^2(r) \left(E^2 - f(r) \left(\frac{\ell^2}{r^2} \right) \right)} + \frac{aN\ell}{E} - \frac{aN\ell}{2Ef(r) \left(E^2 - f(r) \left(\frac{\ell^2}{r^2} \right) \right)} \right] \times f^2(r) \sqrt{E^2 - f(r) \left(\frac{\ell^2}{r^2} \right)}, \quad (3.5.1)$$

replace $N = \frac{2M}{r^3}$ in the given equation then we have

$$v = \left[1 - \frac{1}{2f(r)\left(E^2 - f(r)\left(\frac{\ell^2}{r^2}\right)\right)} - \frac{2aM\ell E}{r^3 f^2(r)\left(E^2 - f(r)\left(\frac{\ell^2}{r^2}\right)\right)} + \frac{2aM\ell}{r^3 E} - \frac{aM\ell}{r^3 E f(r)\left(E^2 - f(r)\left(\frac{\ell^2}{r^2}\right)\right)} \right] \times f^2(r) \sqrt{E^2 - f(r)\left(\frac{\ell^2}{r^2}\right)}. \quad (3.5.2)$$

We have two cases which are

3.5.1 Timelike Geodesic for Radial Motion of the Particle

By putting $\ell = 0$, then equation (3.5.2) becomes

$$v = f^2(r) \left(1 - \frac{1}{2f(r)E^2} \right), \quad (3.5.3)$$

putting $E = 1$ and $f(r)$ value, we get

$$v = \left(1 + \omega r^2 - \sqrt{r(\omega^2 r^3 + 4\omega M)} \right)^2 \left(1 - \frac{1}{2(1 + \omega r^2 - \sqrt{r(\omega^2 r^3 + 4\omega M)})} \right). \quad (3.5.4)$$

Figure (3.21) and (3.22): A geodesics sketch for radial motion of the particle bounce back scenario. These graphs reveal that an ingoing particle comes from infinity with some velocity, reaches to a limit (dashed line) and then bounces back to infinity. Where dashed line is the boundary that does not allow the particle to cross that limit.

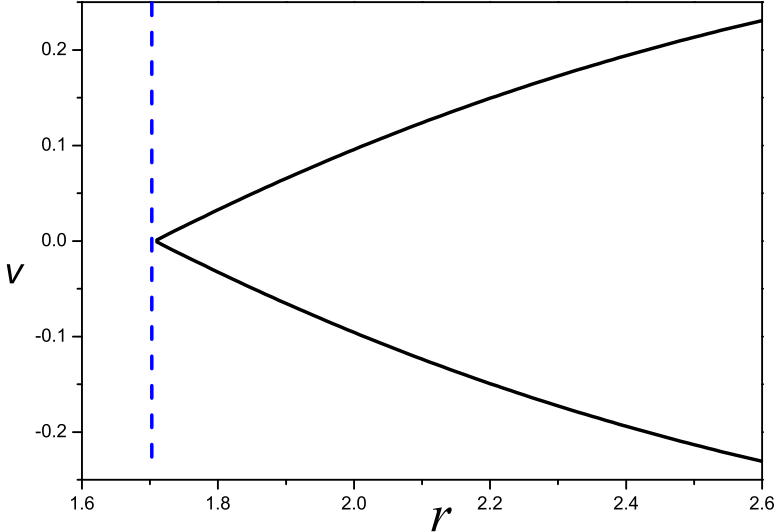


Figure 3.21: Graph of v vs r with parameters $\omega = 1$ and $M = 1$ for equation (3.5.4)

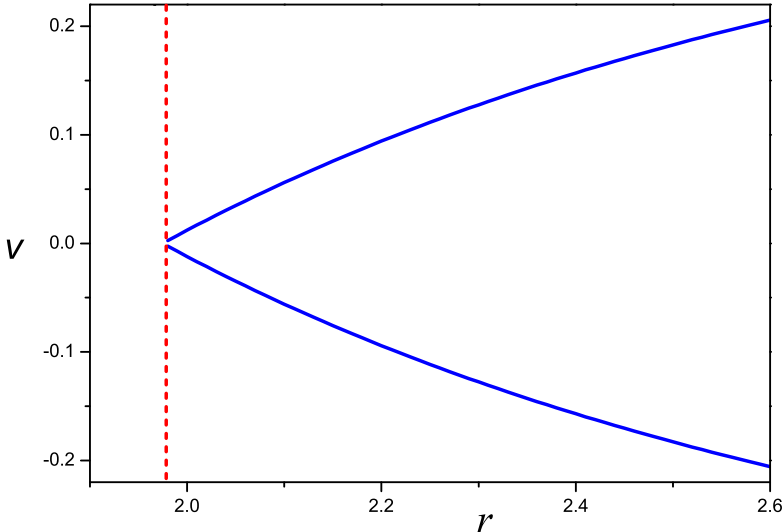


Figure 3.22: Graph of v vs r with parameters $\omega = 10$ and $M = 1$ for equation (3.5.4)

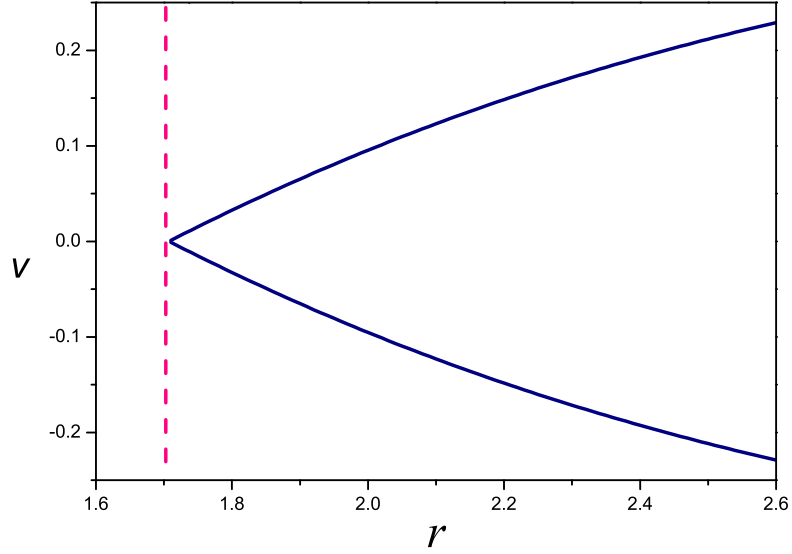


Figure 3.23: Graph of v vs r with parameters $\ell = 0.5$, $\omega = 1$, $M = 1$ and $E = 1$ and $a = 0.5$ for equation (3.5.5)

3.5.2 Timelike Geodesic for Non-radial Motion of the Particle

Put $\ell \neq 0$ in equation (3.5.2) and then simplifying we get

$$\begin{aligned}
 v = & \left[1 - \frac{1}{2f(r)\left(E^2 - f(r)\left(\frac{\ell^2}{r^2}\right)\right)} - \frac{2aM\ell E}{r^3 f^2(r)\left(E^2 - f(r)\left(\frac{\ell^2}{r^2}\right)\right)} \right. \\
 & \left. + \frac{2aM\ell}{r^3 E} - \frac{aM\ell}{r^3 E f(r)\left(E^2 - f(r)\left(\frac{\ell^2}{r^2}\right)\right)} \right] \times \\
 & f^2(r) \sqrt{E^2 - f(r)\left(\frac{\ell^2}{r^2}\right)}. \tag{3.5.5}
 \end{aligned}$$

Figure (3.23) and (3.24): Here the geodesics show the path for radial motion of the particle. In these sketches the particle comes from infinity having some initial velocity, reaching to a limit (boundary beyond which the particle can not go) denoted by dashed line. And then

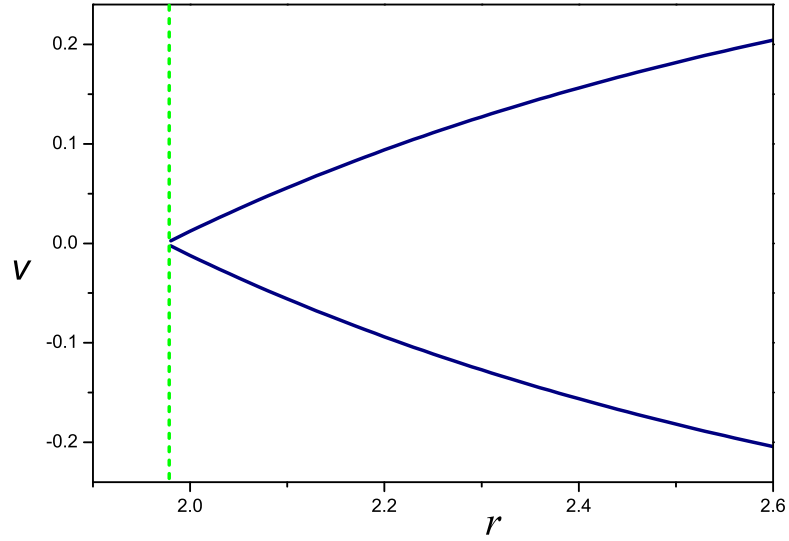


Figure 3.24: Graph of v vs r with parameters $\ell = 0.5$, $M = 1$ and $E = 1$, $\omega = 10$ and $a = 0.5$ for equation (3.5.5)

going back to infinity again as given per figure.

3.6 Null Geodesics

Insert $h = 0$ and value of shift function in equation (3.4.6) we obtain

$$v = f^2(r) \sqrt{E^2 - f(r) \left(\frac{\ell^2}{r^2} \right)} \left[1 - \frac{2aM\ell E}{r^3 f^2(r) \left(E^2 - f(r) \left(\frac{\ell^2}{r^2} \right) \right)} + \frac{2aM\ell}{r^3 E} \right] \left[E^{-1} \right]. \quad (3.6.1)$$

From here again we have two case

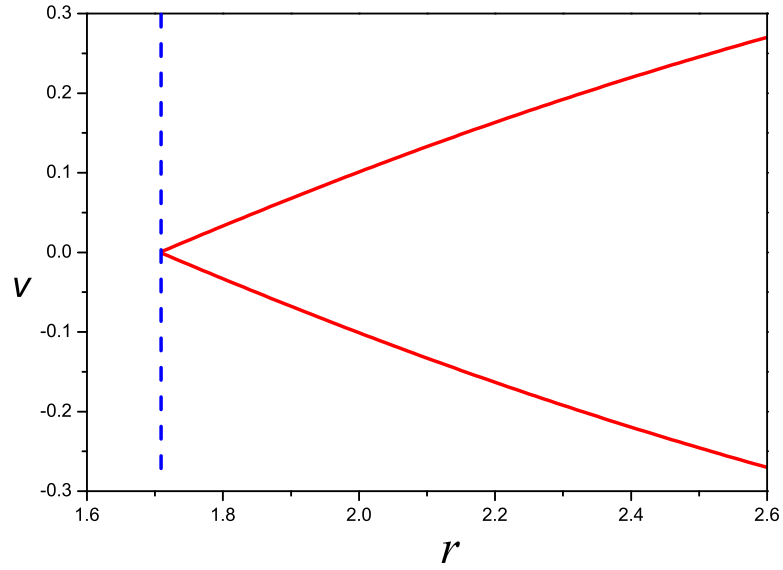


Figure 3.25: Graph of v vs r with parameters $\omega = 1$, $M = 1$ for equation (3.6.2)

3.6.1 Null Geodesic for Radial Motion of the Particle

When $\ell = 0$ the expression (3.6.1) becomes $v = f(r)$. In this case the velocity equals to lapse function which is

$$v = \left(1 + \omega r^2 - \sqrt{r(\omega^2 r^3 + 4\omega M)} \right)^2. \quad (3.6.2)$$

Figure (3.25) and (3.26): In the given graphs geodesics represents the trajectory for radial motion of the particle coming from infinity with some initial velocity and then bounces back to infinity.

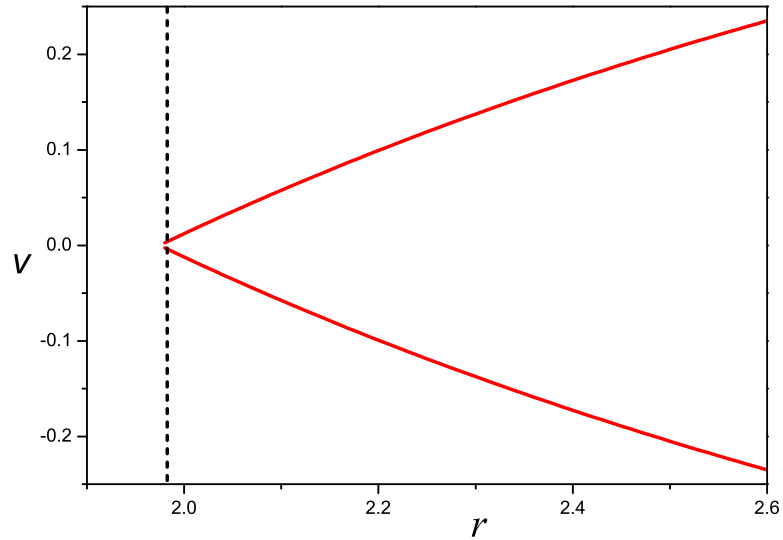


Figure 3.26: Graph of v vs r with parameters $\omega = 10$, $M = 1$ for equation (3.6.2)

3.6.2 Null Geodesic for Non-radial Motion of the Particle

Put $\ell \neq 0$ in equation (3.6.1) we get

$$v = f^2(r) \sqrt{E^2 - f(r) \left(\frac{\ell^2}{r^2} \right)} \left[1 - \frac{2aM\ell E}{r^3 f^2(r) \left(E^2 - f(r) \left(\frac{\ell^2}{r^2} \right) \right)} + \frac{2aM\ell}{r^3 E} \right] \left[E^{-1} \right]. \quad (3.6.3)$$

Figure (3.27) and (3.28): These graphs reflect that the particle comes from infinity and going back to infinity, by making the geodesics path as shown per figure.

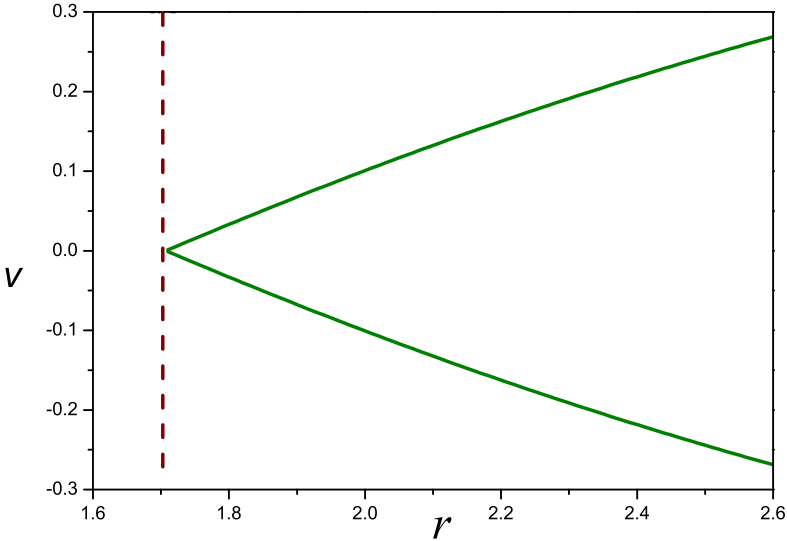


Figure 3.27: Graph of v vs r with parameters $\omega = 1$, $M = 1$, $\ell = 0.5$ and $a = 0.5$ for equation (3.6.3)

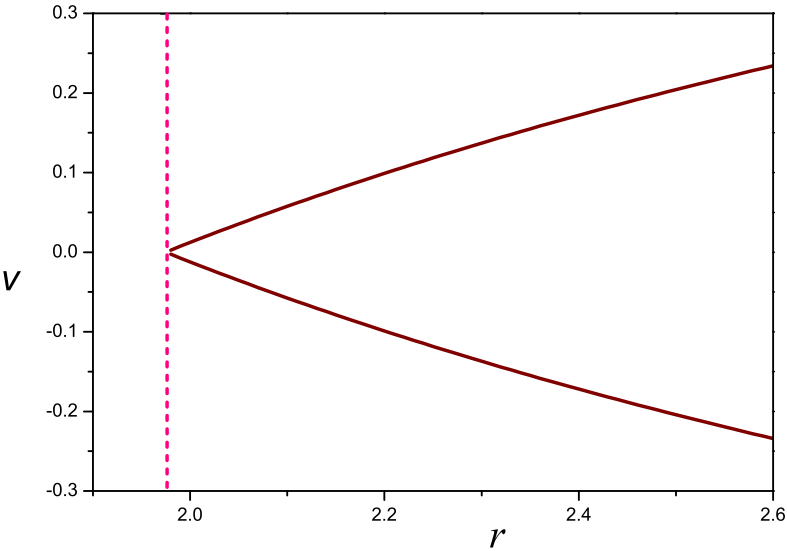


Figure 3.28: Graph of v vs r with parameters $\omega = 10$, $M = 1$, $\ell = 0.5$, $\ell = 0.5$ and $a = 0.5$ for equation (3.6.3)

Chapter 4

Conclusion

We have discussed the null and timelike geodesic motion for radial and non-radial motion of particles in the vicinity of a slowly rotating Hořava Lifshitz Black hole [38]. By examining the effective potential behaviour for the particle, we worked out the timelike geodesic motion of particle in static Hořava- Lifshitz spacetime. When energy of the particle is in proper range then the particle comes from finite distance to the center along timelike geodesics. However the complexity arises in the case of the radial motion of the particle along timelike geodesics. Therefore we have the following cases for the energy of the radial motion of the particle: If ‘ E ’ (energy of the particle) is greater than the critical energy value E_C , then the particle directly jumps from infinity into singularity. If energy of the particle ‘ E ’ becomes equal to the critical energy value E_C , the particle’s orbit become unstable at $r = r_C$. It means that the particle goes to infinity or singularity from $r = r_C$. If energy ‘ E ’ of the particle is in appropriate range the particle redirect to infinity or goes to singularity from infinity.

When we compared results of timelike geodesic motion for radial and non-radial motion of the particle in slowly rotating Hořava-Lifshitz black hole spacetime with that of static Hořava-Lifshitz black hole spacetime we deduce that the dynamics of the particles affects. Similarly the behaviour of effective potential for radial and non-radial motion of the particle

was also studied graphically in slowly rotating Hořava-Lifshitz spacetime. We arrived at the fact that by involving the spin term in the static Hořava Lifshitz spacetime metric there is no such difference occur between static Hořava-Lifshitz spacetime [28] and slowly rotating Hořava-Lifshitz black hole. The difference occurs only in maxima of the effective potential, it means that only instability of the orbit of the particle changes. From this research work we proved that if we introduce the spin term in the static Hořava-Lifshitz spacetime metric, the instability of the particle increases.

Bibliography

- [1] A. Qadir, *General Theory of Reativity*, (unpublished).
- [2] S. Chandrasekher, *The Mathematical Theory of Black Holes* (Oxford, England 1983).
- [3] T. P. Cheng, *Gravitation and Cosmology* (Oxford University Press, 2005).
- [4] R. M. Wald, *General Relativity* (Chicago University Press, London 1984).
- [5] S. Loibe, K. Shibata, T. Kudoh and D. L. Meier, *Science* **295**, 1688-1691 (2002).
- [6] Rhoades, E. J. Clifford, R. Ruffni, *Phys. Rev. Lett.* **32**, 324 (1974).
- [7] M. P. Hobson, G. P. Efstathiou and A. N. Lasenby, *General Relativity: An Introduction for Physicists* (Cambridge University Press, 2006).
- [8] J. B. Hartle, *An Introduction to Einstein's General Relativity* (Addison-Wesley, San Francisco, 2003).
- [9] B. Schutz, *A First Course in General Relativity* (Cambridge University Press, 2009).
- [10] R. Ruffni and J. A. Wheeler, *Physics Today* 30-41 (1971).
- [11] P. Hořava, *Phys. Rev. Lett.* **102**, 161301 (2009).
- [12] J. Chen and Y. Wang, *Int. J. Mod. Phys. A* **25**, 1439 (2010).
- [13] J. Sadeghi, B. Pourhassan, *Eur. Phys. J. C. Theor. Phys.* **72**, 1984 (2012).

- [14] O. Gron and S. Harvik, *Einstein's General Theory of Relativity* (Springer New York, 2007).
- [15] C. W. Misner, K. S. Thorne and J. A. Wheeler, *Gravitation* (San Francisco, 1973).
- [16] Committee on Gravitational Physics, Board on Physics and Astronomy, Commission on physical Sciences, Mathematics and Applications, National Research Council, *Gravitational Physics, Exploring the Structure of Space and Time* (unpublished).
- [17] S. Hawking, *A Brief History of Time*, (London, 1988).
- [18] A. A. Siddique, *PhD Thesis* (2002).
- [19] H. Ohanian, R. Ruffini, *Gravitation and Spacetime*, Second Edition (London 1994).
- [20] I. Asimov, *The Collapsing Universe*, (New York 1957).
- [21] F. Melia, *Cracking the Einstein Code*, (Chicago, 2009).
- [22] C. Rovelli, *Quantum gravity*, (Cambridge University Press, 2005).
- [23] S. K. Chakrabarti, K. Dutta, A. A. Sen, arXiv:1108.2781v2 [astro-ph].
- [24] G. Calcagni, JHEP **0909**, 112 (2009).
- [25] A. Kehagias and K. Sfetsos, Phys. Lett. B **678**, 123 (2009).
- [26] H. Lu, J. Mei and C. N. Pope, Phys. Rev. Lett. **103**, 091301 (2009).
- [27] R. G. Cai, B. Hu, H. B. Zhang, Phys. Rev. D **80**, 041501(R) (2009).
- [28] I. Hussain, M. Jameel, B. Majeed, Int. J. Theor. Phys. **54**, 1567-1577 (2015).
- [29] Frolov, Valeri P. Phys.Rev. D **85**, 024020 (2012).
- [30] W. Han, Gen Relativ Gravit **40**, 1831-1847 (2008).
- [31] D. Pugliese, H. Quevedo, R. Ruffini, Phys. Rev. **D83**, 024021 (2011).

- [32] D. Pugliese, H. Quevedo, R. Ruffini, Phys. Rev. **D83**, 104052 (2011).
- [33] O. Luongo and H. Quevedo, arXiv:1430.1507v2 [gr-qc].
- [34] A. García1, E. Hackmann, J. Kunz, C. Lämmerzahl, A. Macias, arXiv:1306.2549v3 [gr-qc].
- [35] A. Abdujabbarov, B. Ahmedov, Phys. Rev. D **84** 044044 (2011).
- [36] A. Abdujabbarov, B. Ahmedov and N. B. Jurayeva, Phys. Rev. D **87**, 064042 (2013).
- [37] A. Kehagious, K. Sfetsos, *The black hole and FRW geometries of non-relativistic gravity*. Phys. Lett. B **678**, 123 (2009).
- [38] M. Jameel, S. Hussain, B. Majeed, Eur. Phys. J. C. Theor. Phys. **05**, 147 (2015).
- [39] I. Radinschi, F. Rahaman, A Banarjee, Int. J. Theor.Phys. **50**(9), 2906-2916 (2011).